Meccanica (2017) 52:2503–2526
DOI 10.1007/s11012-016-0601-1

Control of nonlinear vibrations using the adjoint method

Carmine M. Pappalardo · Domenico Guida

Received: 2 May 2016 / Accepted: 19 December 2016 / Published online: 28 December 2016

Abstract In this paper, a new methodology is proposed to address the problems of suppressing structural vibrations and attenuating contact forces in nonlinear mechanical systems. The computational algorithms developed in this work are based on the mathematical framework of the calculus of variation and take advantage of the numerical implementation of the adjoint method. To this end, the principal aspects of the optimal control theory are reviewed and employed to derive the adjoint equations which form a nonlinear differential-algebraic two-point boundary value problem that defines the mathematical solution of the optimal control problem. The adjoint equations are obtained and solved numerically for the optimal design of control strategies considering a twofold control structure: a feedforward (open-loop) control architecture and a feedback (closed-loop) control scheme. While the feedforward control strategy can be implemented using only the active control paradigm, the feedback control method can be realized employing both the active and the passive control approaches. For this purpose, two dual numerical procedures are developed to numerically compute a set of optimal control policies, namely the adjoint-based control optimization method for feedforward control actions and the adjoint-based parameter optimization method for feedback control actions. The computational methods developed in this work are suitable for controlling nonlinear nonautonomous dynamical systems and feature a broad scope of application. In particular, it is shown in this paper that by setting an appropriate mathematical form of the cost functional, the proposed methods allow for simultaneously solving the problems of suppressing vibrations and attenuating interaction forces for a general class of nonlinear mechanical systems. The numerical example described in the paper illustrates the key features of the adjoint method and demonstrates the feasibility and the effectiveness of the proposed adjoint-based computational procedures.

Keywords Structural vibration suppression · Contact force attenuation · Adjoint method · Optimal control · Feedforward control strategy · Feedback control strategy

C. M. Pappalardo (✉) · D. Guida
Department of Industrial Engineering, University of Salerno, Via Giovanni Paolo II, 132, 84084 Fisciano, Salerno, Italy
e-mail: cpappalardo@unisa.it

1 Introduction

The study of general problems concerning nonlinear vibrations represents an important research area in many fields of engineering and physics [1]. In general, a mechanical system can exhibit a linear or a nonlinear dynamical behavior according to its geometric topology, because of its intrinsic constitutive nature, and

depending on the range over which the external excitations acting on it are specified [2]. Complicated nonlinear behaviors can arise for simple discrete mechanical elements as well as for more complex elastic continuum bodies such as cables, beams, shells, and plates, which represent fundamental components extensively used in different structures and mechanical systems [3]. As a consequence, the development of accurate analytical and numerical techniques for modeling nonlinear mechanical systems represents an important issue that has gained great attention in recent years [4].

Mechanical systems are generally influenced by different energy sources which may potentially excite structural vibrations [5]. The amplitudes of such structural vibrations can span from nanometres, such as in precision engineering machines and mechanisms, to meters, as can occur in civil engineering applications [6]. In aerospace engineering facilities, on the other hand, lightweight structures featuring lightly damped flexible components are commonly employed [7]. Such flexible multibody systems are prone to a vibratory behavior which, in turn, is incompatible with the stringent requirements that need to be satisfied for the purpose of position and orientation control of aircraft [8]. Furthermore, structural vibrations can have significant detrimental effects on the performance of the mechanical system that experiences them and may represent a serious danger for the integrity of the system itself [9]. Therefore, in many engineering applications, the problem of vibration control is of primary importance and a large amount of analytical and numerical research has been devoted to this relevant issue [10].

Many realistic models of mechanical systems are characterized by a nonlinear dynamical behavior that makes the control problem a challenging task [11]. Generally speaking, the control strategies adopted to address this issue can be classified in two vast categories, namely the active control approach and the passive control approach [12]. Active control systems are formed by a programmable control unit, a set of sensors, and an array of actuators. The data collected by the sensors constitute the input signals for the control device. The control unit then analyzes and processes the sensor signals in order to generate the input signals for the control actuators. Finally, the signals outputted from the control device reach the actuators, which act on the mechanical systems, thereby reducing potentially harmful vibrations [13]. Passive control systems, on the other hand, make use of feedback information describing the system state but do not rely on a reprogrammable control device and, therefore, are based on a rigid control scheme [14]. Active control systems for the reduction of nonlinear vibrations feature typically superior performance because they are flexible and reprogrammable but passive control systems are generally more reliable since they are devised to work without any external power supply [15]. Thus, choosing between the main features of the active and the passive control strategies in the design phase of optimal controllers for a nonlinear dynamical system represents a non-trivial task.

Active control systems can be more advantageous than their passive counterparts featuring comparable performances. However, the design of an effective control strategy for a nonlinear mechanical system controlled using the active approach is generally more complex, especially in the case of flexible multibody systems [16]. By employing the active control method, the mechanical vibrations are mitigated by the application of a set of actively controlled forces aimed to contrast the inertia and the elastic forces induced by the external sources of excitation [17]. Adopting the passive control strategy, on the other hand, reduces or suppresses structural vibrations by employing two different methods, namely the vibration isolation and the vibration absorption [18]. The isolation of structural vibrations consists in a proper design of the connection between a mechanical system and the external environment, or the ground, such that the unwanted external disturbances are eliminated or reduced by the connection itself [19]. On the other hand, the absorption of structural vibrations is realized by designing a particular mechanical device capable of absorbing or dissipating the unwanted kinetic energy of the main structural system, as for instance in the case of the dynamic vibration absorbers employed for mechanical and civil engineering applications [20]. Moreover, the control problem for the contact forces is also particularly important in many robotic applications where, for example, a compliant motion is produced by the interaction of the end effector of a robotic manipulator with the surface of a flexible body [21].

The adjoint method is a versatile mathematical tool for solving the optimal control problem in the general

case of nonlinear mechanical systems [22]. The adjoint-based sensitivity analysis encapsulates a large number of mathematical theories, physical concepts and computational methods in a unified framework [23]. Indeed, the adjoint method finds several analytical and numerical applications that span much beyond those originally imagined [24]. From a computational point of view, the prominent feature of the adjoint method is the fact that, in the case of a general dynamical simulation that describes the time evolution of the state of a mechanical system for a complex nonlinear problem, the sensitivity of a predetermined objective quantity with respect to the controlled input data can be effectively computed by a linear adjoint procedure featuring approximately the same computational cost of the original dynamical simulation [25]. On the other hand, in the classical linearization method based on the superposition principle, a set of separate linearized problems has to be independently solved for each increment of the controlled input variables [26, 27]. The main idea behind this approach to the control problem leads also to the dynamic programming method which, in turn, suffers from the important drawback of the so-called curse of dimensionality, namely the dimension and the complexity of the problem grow exponentially with respect to the number of the state variables [28]. Therefore, the linearization method is considerably less general and much slower compared to the adjoint method [29]. Because of its advantageous key properties, the adjoint method has many relevant applications in fluid mechanics, since in this field complex nonlinear problems featuring a large number of degrees of freedom are often the norm [30]. For instance, the adjoint method can be utilized to design an optimal aerodynamic shape that minimizes the drag coefficient for a given lift coefficient [31], it can be used as a numerical technique to extract the receptivity coefficient of a complex flow configuration [32], and it can be employed to perform sensitivity and stability analyses of a base flow subjected to small perturbations [33]. Furthermore, the adjoint method can be successfully employed to deal with linear as well as nonlinear optimal control problems in general. In the case of linear systems, or for linear dynamical models resulting from the linearization process of nonlinear mechanical systems around a given trajectory, several effective algorithms based on the adjoint method were developed for fluid mechanics applications in order to solve large optimal control problems bypassing the solution of the Riccati equations [34]. On the other hand, only recently the adjoint method has been employed in the field of robotics and for the design, optimization, and control of mechanical systems [35, 36]. Thus, the use of the adjoint analysis in the general field of applied mechanics is still at an early stage but, from a mathematical standpoint, it has almost reached the maturity leading to a substantial generalization of the concept of the linear-quadratic regulator method (LQR) to the numerical solution of complex nonlinear control problems, as shown in some fluid mechanics applications [37]. This paper represents an attempt to fill this gap and to pave the way towards a further analytical and computational development of the adjoint-based analysis for controlling rigid and flexible multibody systems characterized by nonlinear differential-algebraic equations of motion.

Over the past thirty years, considerable efforts have been devoted to the design of control strategies for the simultaneous suppression of structural vibrations and attenuation of contact forces in nonlinear mechanical systems [38]. In fact, a crucial aspect of the motion control problem for nonlinear mechanical systems is the capacity to handle the interaction between the system and the external environment [39]. Indeed, the contact forces are physical quantities which characterize the state of interaction of the mechanical system of interest with the external world [40]. One possible approach to deal with this problem is to design specific control strategies which consider a hybrid motion-force control scheme that decouples the motion control and the force control tasks into two subtasks which can be independently accomplished [41]. The adjoint-based optimization algorithm, on the other hand, is a nonlinear control optimization strategy which is extremely suitable to deal with a considerable class of coupled nonlinear optimization problems [42, 43]. Therefore, the main idea behind this investigation is to explore the possibility of addressing the interaction control problem for nonlinear mechanical systems by using an adjoint-based optimization approach.

In this investigation, a novel method is proposed to derive feedforward and feedback control actions for solving the problem of suppressing structural vibrations and attenuating contact forces for nonlinear mechanical systems utilizing two dual general-

purpose computational procedures: the adjoint-based control optimization method and the adjoint-based parameter optimization method. This paper is organized as follows. Section 2 illustrates the main mathematical features of the adjoint method for optimal control design. To this end, a concise review of optimal control theory is reported for both the feedforward and the feedback control strategies, followed by a pointwise description of the nonlinear control and parameter optimization approaches based on the adjoint method. Section 3 examines the control problem for structural vibrations and the simultaneous isolation problem for externally induced interaction forces in the case of an archetypical two degrees of freedom nonlinear mechanical system. For this purpose, the nonlinear equations of motion of the simple dynamical system considered as a case study are readily derived and an appropriate quadratic structure of the cost functional is set in order to mathematically formulate the simultaneous control problems for suppressing structural vibrations and attenuating contact forces in the context of the optimal control theory. This derivation is meant to show how to explicitly obtain the sensitivity vectors and matrices necessary for the computer implementation of the adjoint-based optimization procedures proposed in the paper. Subsequently, in this section, the synthesis of two types of control strategies, namely a feedforward controller and a feedback controller, is provided together with the corresponding evolution of the system state and of the interaction force. Some quantitative metrics arising from the numerical results obtained in the paper are also shown in this section to demonstrate the effectiveness of the implementation of the control methods developed in this investigation. Finally, Sect. 4 includes a summary and the conclusions of the paper.

2 Adjoint method for optimal control design

In this section, the basic elements of the optimal control theory and the practical implementation of the adjoint method are briefly reviewed. To this end, the necessary conditions that arise from the analytical solution of the optimal control problem for continuous-time dynamical systems are derived considering two general cases, namely an optimal feedforward controller and an optimal feedback controller. Subsequently, the computational algorithms for the implementation of the adjoint-based control optimization method and, respectively, of the adjoint-based parameter optimization method are discussed.

2.1 Design of an optimal feedforward controller

In this subsection, the necessary conditions that identify the analytical solution of the optimal control problem are developed employing some mathematical techniques borrowed from the calculus of variation theory like, for instance, the fundamental theorem of the calculus of variation. In particular, the differential-algebraic equations that produce an optimal feedforward control action are derived exploiting the Pontryagin minimum principle.

A feedforward or open-loop controller is a control policy determined as an explicit function of time and of the specific initial conditions of the dynamical system under examination [44]. Consider a set of n nonlinear differential equations which describes the state evolution of a continuous-time dynamical system:

$$\begin{cases} \dot{\mathbf{z}} = \mathbf{N} \\ \mathbf{z}|_{t=0} = \mathbf{z}_0 \end{cases} \tag{1}$$

where t is time, $\mathbf{z} \equiv \mathbf{z}(t)$ denotes a n-dimensional vector representing the system state, $\mathbf{z}_0$ is a n-dimensional vector representing the system initial conditions, $\mathbf{N} \equiv \mathbf{N}(t, \mathbf{z}, \mathbf{u}, \mathbf{r})$ identifies a n-dimensional vector function that regulates the time evolution of the system state, $\mathbf{u} \equiv \mathbf{u}(t)$ is a m_u-dimensional vector of feedforward control actions and $\mathbf{r} \equiv \mathbf{r}(t)$ denotes a m_r-dimensional vector of external inputs. The vector function $\mathbf{N}$ represents a set of n nonlinear ordinary differential equations that mathematically describes the dynamics of the continuous-time system or plant to be controlled. On the other hand, assume a scalar cost functional $J \equiv J(\mathbf{z}_0)$ featuring the following analytical form:

$$J = h|_{t=T} + \int_0^T g \mathrm{d}t \tag{2}$$

where T is a fixed time domain for the control actuation, $h \equiv h(t, \mathbf{z}, \tilde{\mathbf{z}})$ is a scalar function that identifies the terminal cost function, $g \equiv g(t, \mathbf{z}, \tilde{\mathbf{z}}, \mathbf{u}, \tilde{\mathbf{u}}, \mathbf{r}, \tilde{\sigma})$ is a scalar function that denotes the current cost function, $\tilde{\mathbf{z}} \equiv \tilde{\mathbf{z}}(t)$ is a n-dimensional

vector representing a preassigned reference state trajectory, $\tilde{\mathbf{u}} \equiv \tilde{\mathbf{u}}(t)$ is a m_u-dimensional vector representing a precomputed reference control action and $\tilde{\sigma} \equiv \tilde{\sigma}(t)$ is an l-dimensional vector representing an assumed reference interaction vector. Without loss of generality, the reference functions $\tilde{\mathbf{z}}$, $\tilde{\mathbf{u}}$ and $\tilde{\sigma}$ are typically set equal to zero vectors in the case of regulation problems whereas in tracking problems these functions result from the numerical solution of a previously solved motion planning problem [45]. It is important to note that the performance index J is selected by the analyst in order to make the plant exhibit a desired type of dynamical behaviour. In fact, the cost functional J is a mathematical entity which reflects how well a specific control law $\mathbf{u}$ meets the design goals and, therefore, it is employed as a metric to quantitatively assess the performances of a dynamical system subjected to a particular set of control actions. Thus, in the case of a feedforward controller, the optimal control problem consists of finding an optimal feedforward control action $\mathbf{u}^* \equiv \mathbf{u}^*(t)$ which causes the dynamical system to follow an optimal trajectory $\mathbf{z}^* \equiv \mathbf{z}^*(t)$ that corresponds to a global minimum of the cost functional $J^* \equiv J^*(\mathbf{z}_0)$ [46]. In other words, from a mathematical point of view, the problem at hand for the feedforward optimal control is to find the minimum of the cost functional (2) subjected to a set of differential constraint equations which represents analytically the system dynamical model (1). Thus, the key idea to solve this challenging mathematical problem is to consider the system dynamical model as a set of differential constraint equations for the minimization problem under consideration and, therefore, the adjoint method can be employed to define an augmented cost functional $\bar{J} \equiv \bar{J}(\mathbf{z}_0)$. To this end, the system state-space equations of motion (1) can be adjoined to the cost functional (2) in order to obtain an augmented cost functional defined as follows:

$$\bar{J} = h|_{t=T} + \int_0^T g + \lambda^T(\mathbf{N} - \dot{\mathbf{z}})\mathrm{d}t \tag{3}$$

where $\lambda \equiv \lambda(t)$ defines a costate or adjoint state vector which identifies the Lagrange multipliers resulting from the adjoining process of the system equations of motion to the cost functional. An effective method to address the problem under study is to resort to the Pontryagin minimum principle. In order to simplify the mathematical derivation of the necessary equations which lead to the minimum of the augmented cost functional (3), a Hamiltonian function $H \equiv H(t, \mathbf{z}, \tilde{\mathbf{z}}, \mathbf{u}, \tilde{\mathbf{u}}, \mathbf{r}, \tilde{\sigma})$ can be utilized. The Hamiltonian function H is defined as:

$$H = g + \lambda^T \mathbf{N} \tag{4}$$

According to the Pontryagin minimum principle, an optimal control action $\mathbf{u}^* \equiv \mathbf{u}^*(t)$ produces an optimal state trajectory $\mathbf{z}^* \equiv \mathbf{z}^*(t)$ that corresponds to an unconstrained minimum of the Hamiltonian function $H^* \equiv H^*(t, \mathbf{z}^*, \tilde{\mathbf{z}}, \mathbf{u}^*, \tilde{\mathbf{u}}, \mathbf{r}, \tilde{\sigma})$ [47]. Hence, using the definition of the Hamiltonian function (4), the augmented cost functional (3) can be rewritten as:

$$\bar{J} = h|_{t=T} + \int_0^T H - \lambda^T \dot{\mathbf{z}}\mathrm{d}t \tag{5}$$

The augmented cost functional $\bar{J}$ can be reformulated by using the integration by parts rule in order to explicitly obtain the time derivative of the adjoint state λ as follows:

$$\bar{J} = h|_{t=T} - \lambda^T \mathbf{z}\big|_{t=T} + \lambda^T \mathbf{z}\big|_{t=0} + \int_0^T H + \dot{\lambda}^T \mathbf{z}\mathrm{d}t \tag{6}$$

By virtue of the fundamental theorem of the calculus of variation, the variation of the augmented cost functional $\bar{J}$ vanishes on an extremal state trajectory $\mathbf{z}^*$ caused by an extremal control policy $\mathbf{u}^*$ [48]. Indeed, the first variation of the augmented cost functional $\bar{J}$ with respect to the system state $\mathbf{z}$ and with respect to the control action $\mathbf{u}$ yields:

$$\begin{aligned}\delta\bar{J} = &\left(\left(\frac{\partial h}{\partial \mathbf{z}}\right)^T - \lambda\right)^T \delta\mathbf{z}\bigg|_{t=T} + \lambda^T \delta\mathbf{z}\big|_{t=0} \\ &+ \int_0^T \left(\left(\frac{\partial H}{\partial \mathbf{z}}\right)^T + \dot{\lambda}\right)^T \delta\mathbf{z} + \frac{\partial H}{\partial \mathbf{u}}\delta\mathbf{u}\mathrm{d}t\end{aligned} \tag{7}$$

The mathematical form of the variation of the augmented cost functional (7) can be considerably simplified introducing the following definitions:

$$\begin{cases} \mathbf{A} = \dfrac{\partial \mathbf{N}}{\partial \mathbf{z}}, & \mathbf{B} = \dfrac{\partial \mathbf{N}}{\partial \mathbf{u}} \\ v = \dfrac{\partial h}{\partial \mathbf{z}}, & \varphi = \dfrac{\partial g}{\partial \mathbf{z}}, \qquad \psi = \dfrac{\partial g}{\partial \mathbf{u}} \end{cases} \tag{8}$$

where $\mathbf{A} \equiv \mathbf{A}(t, \mathbf{z}, \mathbf{u}, \mathbf{r})$ is a $n \times n$ matrix that represents the sensitivity of the system state function $\mathbf{N}$ with respect to the system state $\mathbf{z}$, $\mathbf{B} \equiv \mathbf{B}(t, \mathbf{z}, \mathbf{u}, \mathbf{r})$ denotes a $n \times m_u$ matrix representing the sensitivity of the system state function $\mathbf{N}$ with respect to the control action $\mathbf{u}$, $v \equiv v(t, \mathbf{z}, \tilde{\mathbf{z}})$ identify a n-dimensional vector that describes the sensitivity of the terminal cost function h with respect to the state vector $\mathbf{z}$, $\varphi \equiv \varphi(t, \mathbf{z}, \tilde{\mathbf{z}}, \mathbf{u}, \tilde{\mathbf{u}}, \mathbf{r}, \tilde{\sigma})$ is a n-dimensional vector describing the sensitivity of the current cost function g with respect to the system state $\mathbf{z}$ and $\psi \equiv \psi(t, \mathbf{z}, \tilde{\mathbf{z}}, \mathbf{u}, \tilde{\mathbf{u}}, \mathbf{r}, \tilde{\sigma})$ is a m_u-dimensional vector that denotes the sensitivity of the current cost function g with respect to the control vector $\mathbf{u}$. By using the definitions of the system sensitivity matrices and vectors provided by the Eq. (8), the variation of the augmented cost functional (7) can be rewritten as:

$$\begin{aligned}\delta\bar{J} &= \left(v^T - \lambda\right)^T \delta\mathbf{z}\Big|_{t=T} + \lambda^T \delta\mathbf{z}|_{t=0} \\ &\quad + \int_0^T \left(\varphi^T + \mathbf{A}^T\lambda + \dot{\lambda}\right)^T \delta\mathbf{z} + \left(\psi^T + \mathbf{B}^T\lambda\right)^T \delta\mathbf{u}\mathrm{d}t \\ &= \left(v^T - \lambda\right)^T \delta\mathbf{z}\Big|_{t=T} + \lambda^T \delta\mathbf{z}|_{t=0} \\ &\quad + \int_0^T \left(\varphi^T + \mathbf{A}^T\lambda + \dot{\lambda}\right)^T \delta\mathbf{z}\mathrm{d}t + \int_0^T \left(\psi^T + \mathbf{B}^T\lambda\right)^T \delta\mathbf{u}\mathrm{d}t = 0\end{aligned} \tag{9}$$

Finally, assuming that the system initial state $\mathbf{z}_0$ is given and considering a fixed time horizon T, the necessary conditions which identify an optimal feedforward controller can be derived setting equal to zero the coefficients of the first variation of the augmented cost functional $\bar{J}$ with respect to the system state $\mathbf{z}$ and with respect to the control action $\mathbf{u}$ as follows:

$$\begin{cases} \dot{\mathbf{z}} = \mathbf{N}, \quad \mathbf{z}|_{t=0} = \mathbf{z}_0 \\ -\dot{\lambda} = \varphi^T + \mathbf{A}^T\lambda, \quad \lambda|_{t=T} = v^T|_{t=T} \\ \psi^T + \mathbf{B}^T\lambda = \mathbf{0} \end{cases} \tag{10}$$

The resulting differential-algebraic equations given by (10) constitute a nonlinear two-point boundary value problem and represent the necessary conditions which define the minimum of the augmented cost functional $\bar{J}$ [49]. In particular, the first vector equation of the set (10) mathematically describes the direct problem, namely the dynamical evolution of the system state $\mathbf{z}$ based on the system initial conditions, whereas the second vector equation of the set (10) mathematically represents the adjoint problem, namely the dynamical evolution of the adjoint state λ based on the corresponding set of boundary or terminal conditions. On the other hand, the third vector equation of the set (10) is called the stationarity equation and defines the minimum of the Hamiltonian function H. It is important to note that the nonlinear ordinary differential equations representing the direct problem, the linear ordinary differential equations that characterize the adjoint problem, and the linear algebraic equations which identify the stationarity conditions are highly coupled and form a nonlinear differential-algebraic two-point boundary value problem. In general, these problems are challenging to solve analytically. However, there are some numerical procedures that can be effectively used to solve this type of mathematical problems. For instance, among the gradient-based optimization techniques, the iterative adjoint-based control optimization algorithm is an efficient and effective computational method capable of designing feedforward control actions for nonlinear mechanical systems [50]. On the other hand, since the adjoint analysis represents a general framework rather than a specific implementation procedure, the adjoint-based control optimization algorithm is the first numerical method developed in this paper.

2.2 Design of an optimal feedback controller

The analytical results derived above are mirrored hereinafter in order to develop an optimal feedback controller. In fact, in this subsection, the necessary conditions that yield an optimal feedback control action are derived exploiting again the Pontryagin minimum principle.

A feedback or closed-loop controller is a control policy determined as an explicit function of the state of the dynamical system examined [51]. Consider a m_u-dimensional vector of feedback control actions denoted with $\mathbf{u} \equiv \mathbf{u}(t, \mathbf{z}; \gamma)$ whose structure depends on the constant m_γ-dimensional parameter vector γ. The parameter vector γ contains a set of coefficients that define a pre-established structure of the feedback control action $\mathbf{u}$, such as a constant feedback structure that depends linearly on the system state $\mathbf{z}$. Hence, in the case of a feedback controller, the optimal control problem consists of finding an optimal set of

parameters γ^* that defines the structure of an optimal feedback control action $\mathbf{u}^* \equiv \mathbf{u}^*(t, \mathbf{z}^*; \gamma^*)$ which causes the dynamical system to follow an optimal trajectory $\mathbf{z}^* \equiv \mathbf{z}^*(t)$ that corresponds to a global minimum of the cost functional $J^* \equiv J^*(\mathbf{z}_0)$ [52]. According to the Pontryagin minimum principle, an optimal set of parameters γ^* defines an optimal control action $\mathbf{u}^* \equiv \mathbf{u}^*(t, \mathbf{z}^*; \gamma^*)$ that yields an optimal state trajectory $\mathbf{z}^* \equiv \mathbf{z}^*(t)$ which identifies an unconstrained minimum of the Hamiltonian function $H^* \equiv H^*(t, \mathbf{z}^*, \tilde{\mathbf{z}}, \mathbf{u}^*, \tilde{\mathbf{u}}, \mathbf{r}, \tilde{\sigma}; \gamma^*)$ [53]. To this end, define:

$$\begin{cases} \mathbf{A} = \dfrac{\partial \mathbf{N}}{\partial \mathbf{z}}, & \mathbf{B} = \dfrac{\partial \mathbf{N}}{\partial \gamma} \\ v = \dfrac{\partial h}{\partial \mathbf{z}}, & \varphi = \dfrac{\partial g}{\partial \mathbf{z}}, \qquad \psi = \dfrac{\partial g}{\partial \gamma} \end{cases} \tag{11}$$

where $\mathbf{A} \equiv \mathbf{A}(t, \mathbf{z}, \mathbf{u}, \mathbf{r}; \gamma)$ is a $n \times n$ matrix that represents the sensitivity of the system state function $\mathbf{N}$ with respect to the system state $\mathbf{z}$, $\mathbf{B} \equiv \mathbf{B}(t, \mathbf{z}, \mathbf{u}, \mathbf{r}; \gamma)$ denotes a $n \times m_\gamma$ matrix representing the sensitivity of the system state function $\mathbf{N}$ with respect to the vector of control parameters γ, $v \equiv v(t, \mathbf{z}, \tilde{\mathbf{z}}; \gamma)$ identify a n-dimensional vector that describes the sensitivity of the terminal cost function h with respect to the state vector $\mathbf{z}$, $\varphi \equiv \varphi(t, \mathbf{z}, \tilde{\mathbf{z}}, \mathbf{u}, \tilde{\mathbf{u}}, \mathbf{r}, \tilde{\sigma}; \gamma)$ is a n-dimensional vector describing the sensitivity of the current cost function g with respect to the system state $\mathbf{z}$, and $\psi \equiv \psi(t, \mathbf{z}, \tilde{\mathbf{z}}, \mathbf{u}, \tilde{\mathbf{u}}, \mathbf{r}, \tilde{\sigma}; \gamma)$ is a m_γ-dimensional vector that denotes the sensitivity of the current cost function g with respect to the vector of control parameters γ. Considering a given set of initial conditions $\mathbf{z}_0$ and assuming that the time horizon T is fixed, the necessary conditions that define an optimal feedback controller can be obtained by setting the coefficients of the first variation of the augmented cost functional $\bar{J}$ equal to zero with respect to the system state $\mathbf{z}$ and with respect to the parameter vector γ following the same mathematical procedure employed in the previous subsection to give:

$$\begin{cases} \dot{\mathbf{z}} = \mathbf{N}, \quad \mathbf{z}|_0 = \mathbf{z}_0 \\ -\dot{\lambda} = \varphi^T + \mathbf{A}^T \lambda, \quad \lambda|_T = v|_T \\ \int_0^T \psi^T + \mathbf{B}^T \lambda \mathrm{d}t = \mathbf{0} \end{cases} \tag{12}$$

The resulting integro-differential equations given by (12) form a nonlinear two-point boundary value problem [54]. Specifically, the first vector equation of the set (12) mathematically describes the direct problem, while the second vector equation of the set (12) mathematically represents the adjoint problem. On the other hand, the third vector equation of the set (12) is called the stationarity equation. It is important to note that, in the case of the formulation of the optimal control problem for a feedback control architecture, the stationarity equations form a set of integral equations. In general, the nonlinear integro-differential two-point boundary value problems are difficult to solve analytically. Nevertheless, some computational procedures can be effectively employed to solve this type of problem numerically. For instance, the iterative adjoint-based parameter optimization algorithm is an efficient and effective computational method that belongs to the class of gradient-based optimization techniques and is able to derive feedback control actions for a vast class of nonlinear mechanical systems [55]. Inspired by the adjoint analysis framework, the adjoint-based parameter optimization algorithm is the second numerical method developed in this paper.

2.3 Computer implementation of the adjoint-based control optimization procedure

In this subsection, the numerical implementation of the adjoint-based control optimization method is discussed in detail and the complete procedure for the computer implementation of the proposed iterative technique is described step by step. In fact, the variational approach presented in the corresponding previous subsection leads to a nonlinear differential-algebraic two-point boundary value problem that, in general, cannot be solved analytically to obtain an optimal feedforward control law. Therefore, one must resort to numerical methods in order to solve such challenging nonlinear problems. To this end, there are three general classes of computational methods that can be employed to solve the problem at hand numerically, namely the neighboring extremal methods, the quasilinearization methods, and the gradient methods [56]. In particular, the numerical technique presented here belongs to the class of the gradient-based optimization methods and is able to determine

an optimal feedforward control action together with the corresponding state trajectory.

The adjoint-based control optimization method represents an iterative numerical algorithm that can be effectively used to find an approximate solution to the nonlinear differential-algebraic two-point boundary value problem defined by equations (10) which identifies an optimal feedforward controller and the corresponding evolution of the system state. This numerical method originates from the field of computational fluid dynamics and is particularly suitable to compute in an efficient and effective way a set of feedforward control actions for mechanical systems featuring a large number of degrees of freedom. The fundamental idea of this gradient-based method is to cleverly exploit the information of the cost functional gradient, which is known analytically, in order to solve the minimization problem at hand via nonlinear optimization techniques [57]. The stationarity equations are rewritten as follows for the sake of simplicity:

$$\psi^T + \mathbf{B}^T \lambda = \mathbf{0} \tag{13}$$

Indeed, for a general state trajectory corresponding to a non-optimal feedforward control action, the non-zero cost functional gradient can be computed using the stationarity conditions (13) as follows:

$$\mathbf{G} = \psi^T + \mathbf{B}^T \lambda \tag{14}$$

where $\mathbf{G} \equiv \mathbf{G}(t, \mathbf{z}, \tilde{\mathbf{z}}, \mathbf{u}, \tilde{\mathbf{u}}, \mathbf{r}, \tilde{\sigma})$ is a n-dimensional vector that represents the cost functional gradient with respect to the feedforward control action for a given instant of time. For the sake of clarity, the adjoint state equations are rewritten here:

$$\begin{cases} -\dot{\lambda} = \varphi^T + \mathbf{A}^T \lambda \\ \\ \lambda|_{t=T} = \nu^T|_{t=T} \end{cases} \tag{15}$$

Note that in correspondence to a non-optimal feedforward control action $\mathbf{u}$ that yields a non-extremal state trajectory $\mathbf{z}$, the cost functional gradient $\mathbf{G}$ is not a zero vector. Thus, considering a trial time history of the control action $\mathbf{u}^k$, where the superscript k refers to the index of the iterative algorithm, first the system state equations (1) must be solved numerically by using the trial time history of the feedforward control action $\mathbf{u}^k$ and then the system adjoint equations (15) must be solved numerically in order to obtain, respectively, a trial time history of the system state $\mathbf{z}^k$ and a trial time history of the adjoint state λ^k. The numerical solutions $\mathbf{z}^k$ and λ^k obtained following this procedure will satisfy, respectively, the initial conditions and the terminal conditions. Subsequently, considering a general step of the iterative adjoint-based control optimization method, the time histories $\mathbf{z}^k$ and λ^k arising from the numerical procedure will not identify the minimum of the cost functional and, therefore, the norm of the corresponding time history of the cost functional gradient $\mathbf{G}^k$ will be different from zero. The time history of the cost functional gradient $\mathbf{G}^k$ can be computed explicitly from the stationary equations (14) once the time history of the system state $\mathbf{z}^k$ and the time history of the adjoint state λ^k are known as follows:

$$\mathbf{G}^k = \left(\psi^k\right)^T + \left(\mathbf{B}^k\right)^T \lambda^k \tag{16}$$

where ψ^k and $\mathbf{B}^k$ denote respectively the time history of the cost-to-go sensitivity vector with respect to the control action and the time history of the state function sensitivity matrix with respect to the control action, both corresponding to the trial solution $\mathbf{u}^k$. The time history of the cost functional gradient $\mathbf{G}^k$ can be used in an iterative gradient-based optimization algorithm in order to gradually improve the time history of the control action $\mathbf{u}^k$ towards the minimum of the cost functional. Typically, to accomplish this task a line search algorithm is used. In general, the line search strategy leads to three general families of minimization methods, namely the steepest descent method, the conjugate gradient method, and the quasi-Newton method [58]. For this purpose, all the algorithms based on the line search strategy utilise the information of the cost functional gradient $\mathbf{G}^k$ to determine a time history of the descent direction $\mathbf{e}^k$ and search the minimum of the cost functional along this direction. This process starts from the current time history of the control action $\mathbf{u}^k$ and leads to the next time history of the control action $\mathbf{u}^{k+1}$ that corresponds to a lower value of the cost functional. Thus, using a line search method the time history of the control input can be iteratively updated as follows:

$$\mathbf{u}^{k+1} = \mathbf{u}^k + \alpha^k \mathbf{e}^k \tag{17}$$

where α^k is a scalar line parameter which represents the step length corresponding to the current iteration. The minimization algorithms based on a line search

strategy differ from each other on the computational method employed to determine the time history of the descent direction $\mathbf{e}^k$ using the time history of the cost functional gradient $\mathbf{G}^k$. Once the time history of the descent direction $\mathbf{e}^k$ is set, the solution for the step length α^k can be found by employing a minimum search algorithm. That is:

$$\alpha^k = \underset{\alpha}{\operatorname{argmin}}(J) \tag{18}$$

The complete procedure necessary for the implementation of the adjoint-based control optimization method can be summarized as follows:

- Step 1: *Direct Problem Solution* use the current time history of the feedforward control action $\mathbf{u}^k$ (or a trial feedforward control time history $\mathbf{u}^0$ for the first iteration) to integrate the system state-space Eq. (10) numerically forward in time starting from the set of initial conditions $\mathbf{z}|_0 = \mathbf{z}_0$ in order to obtain the current state trajectory $\mathbf{z}^k$. For instance, the explicit or implicit Runge-Kutta methods can be used to accomplish this task.
- Step 2: *Adjoint Problem Solution* use the current state trajectory $\mathbf{z}^k$ to integrate the system adjoint state Eq. (10) numerically backward in time starting from the set of terminal conditions $\lambda|_T = v|_T$ in order to obtain the current adjoint state trajectory λ^k. The explicit or implicit Runge-Kutta methods can be used to accomplish this task as well.
- Step 3: *Gradient Computation* use the current state trajectory $\mathbf{z}^k$ and the current adjoint state trajectory λ^k to compute the current time history of the cost functional gradient $\mathbf{G}^k$ by using its explicit expression which stems from the stationary equations.
- Step 4: *Search Direction Computation* use the current time history of the cost functional gradient $\mathbf{G}^k$ to compute the current time history of the search direction $\mathbf{e}^k$. For instance, the steepest descent method, the conjugate gradient methods (such as the Fletcher–Reeves algorithm, the Polak–Ribiere algorithm, or the Hestenes–Stiefel algorithm), or the quasi-Newton methods (such as the Davidon–Fletcher–Powell algorithm or the Broyden–Fletcher–Goldfarb–Shanno algorithm) can be used to accomplish this task.
- Step 5: *Initial Guess Computation* determine an initial guess for the step length α^0 in order to initialize the minimum search algorithm. For instance, the Taylor series method can be used to accomplish this task.
- Step 6: *Bracketing* use the initial guess for the step length α^0 to bracket the minimum of the cost functional J in an interval a^0, b^0, and c^0 along the time history of the search direction $\mathbf{e}^k$. For instance, the Fibonacci method or the golden section method can be used to accomplish this task.
- Step 7: *Minimization* use the bracketed interval a^0, b^0, and c^0 to minimize the cost functional J along the time history of the search direction $\mathbf{e}^k$ in order to find the corresponding step length α^k and to update the time history of the control action $\mathbf{u}^{k+1}$ using the line search strategy (17). For instance, the Fibonacci search method, the golden section search method, or the Brent search method can be used to accomplish this task. If the selected convergence criteria are not satisfied, restart from step 1. For instance, a tolerance on the absolute value of the difference between the current cost functional value J^k and the past cost functional value J^{k-1} or a tolerance on the norm of current time history of the cost functional gradient $\mathbf{G}^k$ can be used to accomplish this task.

The iterative adjoint-based control optimization method leads to a numerical solution of the nonlinear differential-algebraic two-point boundary-value problem defined by the Eq. (10) which provides the time history of the feedforward control action $\mathbf{u}^*$, the time history of the system state trajectory $\mathbf{z}^*$, and the time history of the adjoint state trajectory λ^* corresponding to a minimum of the cost functional J^*.

2.4 Computer implementation of the adjoint-based parameter optimization procedure

The iterative numerical procedure developed above is mirrored here in order to derive the computer implementation of the adjoint-based parameter optimization method, which is described thoroughly in this subsection. In this case, the proposed numerical strategy employs a particular gradient-based optimization

method capable of computing an optimal feedback control action and the corresponding state trajectory.

The adjoint-based parameter optimization method is an iterative numerical procedure which can be effectively used to find an approximate solution to the nonlinear integro-differential two-point boundary value problem defined by Eq. (12) that identify an optimal feedback controller and the corresponding evolution of the system state. Similarly to its counterpart for the feedforward controller, the key idea of this computational method is to employ the information of the cost functional gradient in order to improve gradually the numerical solution for the feedback control action in an iterative fashion taking advantage of an appropriate nonlinear optimization technique [59, 60]. In this case, the minimization process starts from the current value of the control parameter vector γ^k and leads to the next value of the control parameter vector γ^{k+1} following a line search strategy as:

$$\gamma^{k+1} = \gamma^k + \alpha^k \mathbf{e}^k \tag{19}$$

where in this case α^k is a scalar line parameter which represents the step length corresponding to the current iteration. Once the vector representing the descent direction $\mathbf{e}^k$ is set, the solution for the step length α^k can be found using a minimum search algorithm. That is:

$$\alpha^k = \underset{\alpha}{\operatorname{argmin}}(J) \tag{20}$$

The complete procedure to implement the adjoint-based parameter optimization method can be summarized as follows:

- Step 1: *Direct Problem Solution* use the current parameter vector for the control action γ^k (or a trial parameter vector for the control action γ^0 for the first iteration) to integrate the system state-space Eq. (12) numerically forward in time starting from the set of initial conditions $\mathbf{z}|_0 = \mathbf{z}_0$ in order to obtain the current state trajectory $\mathbf{z}^k$. For instance, the explicit or implicit Runge–Kutta methods can be used to accomplish this task.
- Step 2: *Adjoint Problem Solution* use the current state trajectory $\mathbf{z}^k$ to integrate the system adjoint state Eq. (12) numerically backward in time starting from the set of terminal conditions $\lambda|_T = v|_T$ in order to obtain the current adjoint state trajectory λ^k. The explicit or implicit Runge–Kutta methods can be used to accomplish this task as well.
- Step 3: *Gradient Computation* use the current state trajectory $\mathbf{z}^k$ and the current adjoint state trajectory λ^k to compute the current cost functional gradient $\mathbf{G}^k$ by using its explicit expression which stems from the stationarity equations. For instance, the Newton–Cotes methods or the Gauss–Legendre quadrature methods can be used to accomplish this task.
- Step 4: *Search Direction Computation* use the current cost functional gradient $\mathbf{G}^k$ to compute the current search direction $\mathbf{e}^k$. For instance, the steepest descent method, the conjugate gradient methods (such as the Fletcher–Reeves algorithm, the Polak–Ribiere algorithm, or the Hestenes–Stiefel algorithm), or the quasi-Newton methods (such as the Davidon–Fletcher–Powell algorithm or the Broyden–Fletcher–Goldfarb–Shanno algorithm) can be used to accomplish this task.
- Step 5: *Initial Guess Computation* determine an initial guess for the step length α^0 in order to initialize the minimum search algorithm. For instance, the Taylor series method can be used to accomplish this task.
- Step 6: *Bracketing* use the initial guess for the step length α^0 to bracket the minimum of the cost functional J in an interval a^0, b^0, and c^0 along the search direction $\mathbf{e}^k$. For instance, the Fibonacci method or the golden section method can be used to accomplish this task.
- Step 7: *Minimization* use the bracketed interval a^0, b^0, and c^0 to minimize the cost functional J along the search direction $\mathbf{e}^k$ in order to find the corresponding step length α^k and to update the parameter vector for the control action γ^{k+1} using the line search strategy (19). For instance, the Fibonacci search method, the golden section search method or the Brent search method can be used to accomplish this task. If the selected convergence criteria are not satisfied, restart from step 1. For instance, a tolerance on the absolute value of the difference between the current cost functional value J^k and the past cost functional value J^{k-1} or a tolerance on the norm of the current

cost functional gradient $\mathbf{G}^k$ can be used to accomplish this task.

The iterative adjoint-based parameter optimization method leads to a numerical solution of the nonlinear integro-differential two-point boundary-value problem defined by the Eq. (12) which provides the parameter vector for the feedback control action γ^*, the time history of the system state trajectory $\mathbf{z}^*$, and the time history of the adjoint state trajectory λ^* corresponding to a minimum of the cost functional J^*.

3 Numerical results and discussion

In this section, a simple numerical example is provided in order to illustrate the computer implementation of both the adjoint-based control optimization method and the adjoint-based parameter optimization method. The numerical example analyzed here features a twofold structure so that both the proposed nonlinear optimization techniques can be equally applied to exemplify the implementation of the adjoint method for optimal control design.

3.1 Description of the case study

In this subsection, the mechanical system that serves as an illustrative example for the proposed adjoint-based computational methods is described qualitatively and quantitatively.

The dynamical system considered as case-study is a lumped-parameter nonlinear mechanical system featuring two degrees of freedom and is shown in Fig. 1. In Fig. 1, the first mass is denoted with m_1 and the second mass is denoted with m_2. The displacement of the first mass is represented by the coordinate $x_1 \equiv x_1(t)$ while the displacement of the second mass is represented by the coordinate $x_2 \equiv x_2(t)$. The whole system is subjected to a constant gravitational field whose gravitational acceleration is a_g. The mechanical system under consideration features three elastic components which exert three different force fields. The first elastic component provides a nonlinear stiffness denoted with k_1 and its force field features a degree of nonlinearity represented by η. The cubic nonlinear characteristic of the first elastic component is meant to model in a simple manner the stiffening phenomenon of the first spring. Therefore, the

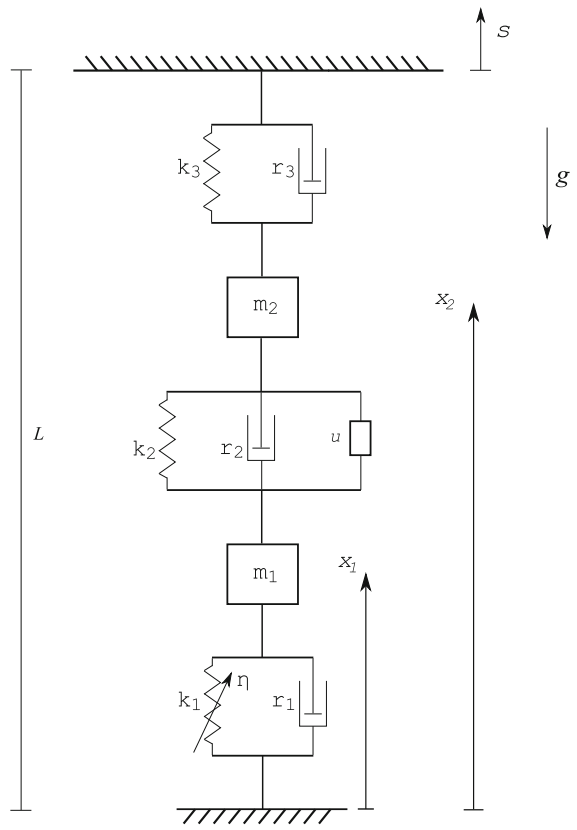

Fig. 1 Mechanical system

nonlinear force field produced by the first elastic component is denoted with $F_{k_1} \equiv F_{k_1}(t, x_1)$ and its structure is assumed as follows:

$$F_{k_1} = -k_1 x_1 \left(1 + \eta x_1^2\right) \tag{21}$$

On the other hand, the second and the third elastic components provide linear elastic force fields whose stiffnesses are denoted respectively with k_2 and k_3. Furthermore, the first, the second, and the third dissipative components shown in Fig. 1 produce three linear dissipative force fields whose damping are represented respectively by the coefficients r_1, r_2, and r_3. The system is hinged on a moving support located at a height L. The displacement of the floating support is identified by the time-dependent variable $s \equiv s(t)$. For the sake of simplicity, its mathematical structure is assumed to be a superposition of two harmonic functions as follows:

$$s = S_1 \sin(2\pi f_1 t) + S_2 \sin(2\pi f_2 t) \tag{22}$$

where S_1 and S_2 denote the amplitudes of the two external displacements while f_1 and f_2 identify respectively the corresponding frequencies of the two harmonic signals. Hence, a control actuator is interposed between the two masses in order to reduce the amplitude of the system vibrations induced by the floating support. To this end, two types of control actions are considered, namely a feedforward controller and a feedback controller. In the case of the feedforward controller, the time-dependent action of the control actuator is denoted with $\mathbf{u} \equiv \mathbf{u}(t)$. In the case of the feedback controller, the state-dependent action of the control actuator is represented by $\mathbf{u} \equiv \mathbf{u}(\mathbf{z}, t; \gamma)$ and a linear structure is assumed as:

$$u = -\gamma_1(x_2 - x_1) - \gamma_2(\dot{x}_2 - \dot{x}_1) \tag{23}$$

where the vector of control parameters γ is defined as follows:

$$\gamma = \begin{bmatrix} \gamma_1 \\ \\ \gamma_2 \end{bmatrix} \tag{24}$$

The linear structure utilized for the feedback controller corresponds to the well-known proportional-derivative feedback control scheme (PD). Indeed, γ_1 denotes the coefficient for the proportional term while γ_2 represents the coefficient of the derivative term for the proportional-derivative feedback controller. Finally, a comprehensive list of all the system data is reported in Table 1.

Table 1 Mechanical system data

Description	Symbols	Data (Units)
First mass	m_1	1 (kg)
Second mass	m_2	2 (kg)
First stiffness	k_1	100 (kg s^{-2})
Second stiffness	k_2	200 (kg s^{-2})
Third stiffness	k_3	300 (kg s^{-2})
First stiffness degree of nonlinearity	η	10 (m^{-2})
First damping	r_1	0.1 (kg s^{-1})
Second damping	r_2	0.2 (kg s^{-1})
Third damping	r_3	0.3 (kg s^{-1})
Gravity acceleration	a_g	9.81 (m s^{-2})
Support height	L	1 (m)
Support displacement—amplitude 1	S_1	0.2 (m)
Support displacement—amplitude 2	S_2	0.04 (m)
Support displacement—frequency 1	f_1	1 (s^{-1})
Support displacement—frequency 2	f_2	10 (s^{-1})
Initial displacement of first mass	$x_{1,0}$	0.01 (m)
Initial displacement of second mass	$x_{2,0}$	0.02 (m)
Initial velocity of first mass	$v_{1,0}$	0.1 (m s^{-1})
Initial velocity of second mass	$v_{2,0}$	0.2 (m s^{-1})

3.2 State-space model of the system equations of motion

In this subsection, the equations of motion of the mechanical system under study are derived and the dynamical model is subsequently represented in the space of the states.

The mechanical system represented in Fig. 1 features $n_2 = 2$ degrees of freedom. Therefore, the system configuration can be easily identified considering a set of two generalized coordinates grouped in a vector $\mathbf{q} \equiv \mathbf{q}(t)$ and defined as:

$$\mathbf{q} = \begin{bmatrix} x_1 \\ \\ x_2 \end{bmatrix} \tag{25}$$

where x_1 and x_2 denote the displacements of the two masses as shown in Fig. 1. Employing the analytical techniques of the Lagrangian mechanics [61, 62], the system equations of motion can be formally written as:

$$\mathbf{M}\ddot{\mathbf{q}} = \mathbf{Q} \tag{26}$$

where $\mathbf{M} \equiv \mathbf{M}(t, \mathbf{q})$ is a $n_2 \times n_2$ matrix representing the system mass matrix and $\mathbf{Q} \equiv \mathbf{Q}(t, \mathbf{q}, \dot{\mathbf{q}}, s, \dot{s})$ is a n_2-dimensional vector denoting the vector of the external generalized forces acting on the system. For the problem at hand, the system mass matrix and the vector of the generalised external forces can be readily derived by using the D'Alemebert-Lagrange principle of virtual work [63, 64]. This well-established method leads to the following mathematical expressions:

$$\mathbf{M} = \begin{bmatrix} m_1 & 0 \\ \\ 0 & m_2 \end{bmatrix} \tag{27}$$

$$\mathbf{Q} = \begin{bmatrix} -m_1 a_g - k_1 x_1 \left(1 + \eta x_1^2\right) - k_2 (x_1 - x_2) - r_1 \dot{x}_1 - r_2 (\dot{x}_1 - \dot{x}_2) \\ -m_2 a_g - k_2 (x_2 - x_1) - k_3 (x_2 - L - s) - r_2 (\dot{x}_2 - \dot{x}_1) - r_3 (\dot{x}_2 - \dot{s}) \end{bmatrix} \tag{28}$$

The system equations of motion (26) form a set of $n_2 = 2$ nonlinear second-order ordinary differential equations which requires a set of $2n_2 = 4$ initial conditions $\mathbf{q}_0$ and $\dot{\mathbf{q}}_0$. When a control action is applied on the system, the system equations of motion changes accordingly as follows:

$$\mathbf{M}\ddot{\mathbf{q}} = \mathbf{Q} + \mathbf{Q}_c \tag{29}$$

where $\mathbf{Q}_c \equiv \mathbf{Q}_c(t, \mathbf{q}, \dot{\mathbf{q}}, u)$ is a n_2-dimensional vector representing the vector of generalized forces arising from the control action. For the system under study, the control action is exerted by a force generated by an actuator acting between the two masses. Thus, in the case of a feedforward controller, the Lagrangian component of the control action $\mathbf{Q}_c$ can be expressed as follows:

$$\mathbf{Q}_c = \begin{bmatrix} -u \\ \\ u \end{bmatrix} \tag{30}$$

On the other hand, in the case of a feedback controller, the Lagrangian component of the control action $\mathbf{Q}_c$ can be written as:

$$\mathbf{Q}_c = \begin{bmatrix} \gamma_1 (x_2 - x_1) + \gamma_2 (\dot{x}_2 - \dot{x}_1) \\ -\gamma_1 (x_2 - x_1) - \gamma_2 (\dot{x}_2 - \dot{x}_1) \end{bmatrix} \tag{31}$$

For the two types of control strategy considered, namely the feedforward control and the feedback control, the controlled system results in an underactuated mechanical system because it features two degrees of freedom but there is only one control input. Underactuated systems represent a general class of dynamical systems particularly challenging to control and, therefore, this kind of mechanical systems is often used to demonstrate the use of novel control methodologies [65, 66]. In order to convert the system equations of motion (26) from the configuration space to the state-space, the system state vector $\mathbf{z}$ can be readily defined as:

$$\mathbf{z} = \begin{bmatrix} \mathbf{q} \\ \\ \dot{\mathbf{q}} \end{bmatrix} = \begin{bmatrix} x_1 \\ \\ x_2 \\ \\ \dot{x}_1 \\ \\ \dot{x}_2 \end{bmatrix} \tag{32}$$

Also, the vector of uncontrollable external actions $\mathbf{r} \equiv \mathbf{r}(t)$ can be written as follows:

$$\mathbf{r} = \begin{bmatrix} s \\ \\ \dot{s} \end{bmatrix} \tag{33}$$

where s and $\dot{s}$ denote respectively the displacement of the moving support and its time derivative. Once the state vector has been defined, the state-space representation of the system dynamical model can be obtained by adding an identity relating the derivative of the configuration vector to the state vector so that the state-space model can be formally written to give:

$$\dot{\mathbf{z}} = \mathbf{N} \tag{34}$$

where $\mathbf{N}$ represents the system state function. The system state-space model (34) constitutes a set of $n = 2n_2 = 4$ nonlinear first-order ordinary differential equations and requires the identification of the initial state $\mathbf{z}_0$ which arises from the set of $n = 2n_2 = 4$ initial conditions $\mathbf{q}_0$ and $\dot{\mathbf{q}}_0$.

3.3 Feedforward control design and development

In this subsection, the adjoint-based control optimization method is employed to design an optimal feedforward controller and the numerical results arising from the implementation of this type of control strategy are shown.

The feedforward controller described here is an open-loop controller designed using the adjoint-based

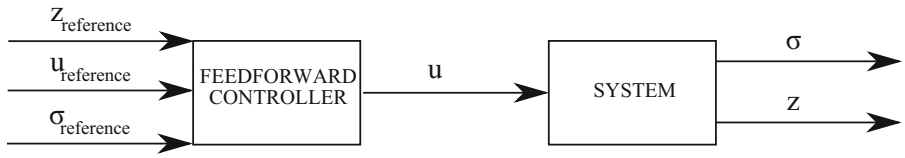

Fig. 2 Control scheme for the feedforward controller

control optimization method. The control scheme which describes how the feedforward controller acts on the mechanical system under study is represented in Fig. 2. The purpose of this feedforward controller is to reduce the amplitudes of the vibrations induced by the moving support and, at the same time, to reduce more drastically the amplitude of the contact force between the second mass and the moving support representing the interaction of the mechanical system with the external environment. For the problem at hand, the contact force σ can be expressed as follows:

$$\sigma = -k_3(L + s - x_2) - r_3(\dot{s} - \dot{x}_2) \tag{35}$$

The terminal cost function h is designed assuming the following quadratic form:

$$h = \frac{1}{2}\mathbf{z}^T\mathbf{Q}_T\mathbf{z} \tag{36}$$

where $\mathbf{Q}_T$ is a diagonal weight matrix which characterises the mathematical structure of the terminal cost function h. On the other hand, the cost-to-go function g is assumed quadratic as well and it is designed.

$$g = \frac{1}{2}\mathbf{z}^T\mathbf{Q}_z\mathbf{z} + \frac{1}{2}\mathbf{u}^T\mathbf{Q}_u\mathbf{u} + \frac{1}{2}\sigma^T\mathbf{Q}_\sigma\sigma \tag{37}$$

where $\mathbf{Q}_z$, $\mathbf{Q}_u$, and $\mathbf{Q}_\sigma$ are diagonal weight matrices which characterise the structure of the cost-to-go function g. The terminal cost sensitivity vector with respect to the system state v can be readily derived by calculating the Jacobian matrix of the terminal cost function h with respect to the system state $\mathbf{z}$. On the other hand, the cost-to-go sensitivity vector with respect to the system state φ can be obtained by computing the Jacobian matrix of the cost-to-go function g with respect to the system state $\mathbf{z}$. The cost-to-go sensitivity vector with respect to the control action ψ can be obtained by deriving the Jacobian matrix of the cost-to-go function g with respect to the control action $\mathbf{u}$. Using the terminal cost sensitivity vector v and the cost-to-go sensitivity vectors ϕ and ψ, the synthesis of a feedforward controller can be performed in order to numerically compute an optimal control action and the corresponding evolution of the system state. The weight matrices which characterise the cost function are set as follows:

$$\begin{cases} \mathbf{Q}_T = diag\left(10^2, 10^2, 10^2, 10^2\right) \\ \mathbf{Q}_z = diag\left(10^2, 10^2, 10^2, 10^2\right) \\ \mathbf{Q}_u = 1 \\ \mathbf{Q}_\sigma = 10^3 \end{cases} \tag{38}$$

Once the necessary system sensitivity matrices and vectors are identified, the adjoint-based control optimization method is implemented in order to derive an optimal feedforward controller following the computational steps described in the paper. To this end, the numerical solutions of the direct problem and of the adjoint problem, which represent steps 1 and 2 of the adjoint-based procedure, are obtained by means of the explicit fourth-order Runge–Kutta method featuring the 3/8-rule. The gradient-based optimization, which represents steps 3 and 4 of the adjoint-based optimization method, is performed using a quasi-Newton method based on the Broyden–Fletcher–Goldfarb–Shanno iterative algorithm. The computation of the initial guess for the minimization procedure, that represents step 5 of the complete algorithm, is realized employing a Taylor series expansion. The bracketing and the minimization for the research of the cost functional minimum, which represent steps 6 and 7 of the proposed computational procedure, are both carried out through the implementation of the Fibonacci search technique featuring a tolerance of 10^{-9} on the relative difference of the cost functional and a tolerance of 10^{-3} for the norm of the cost functional gradient. The numerical integration necessary to evaluate the cost functional corresponding to a given set of control actions is performed using the Simpson method featuring the 3 / 8-rule. The resulting iterative convergence of the cost functional towards the minimum is shown in Fig. 3. This

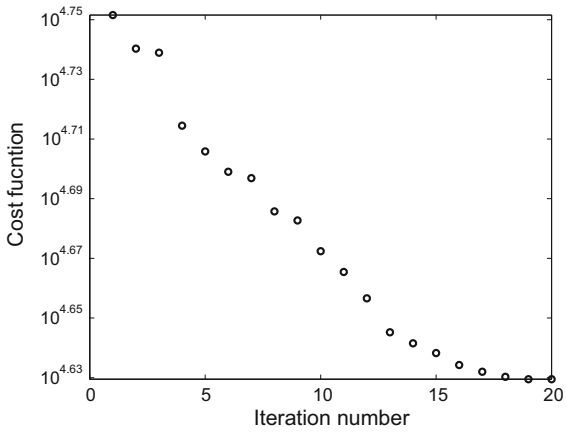

Fig. 3 Cost functional convergence for the feedforward controller—J

figure shows that in this numerical example related to the design of a feedforward control action, the adjoint-based control optimization method features a rapid convergence. The optimal feedforward control action resulting from the adjoint-based control optimization method is depicted in Fig. 4. In Fig. 5 the dashed line depicts the displacement of the first mass when the system is uncontrolled whereas the solid line represents the displacement of the first mass when the feedforward controller acts on the system. In Fig. 6 the dashed line represents the displacement of the second mass when the system is uncontrolled while the solid line depicts the displacement of the second mass when the feedforward controller acts on the system. Qualitatively, these figures show that the effect of the feedforward control action is a considerable amplitude

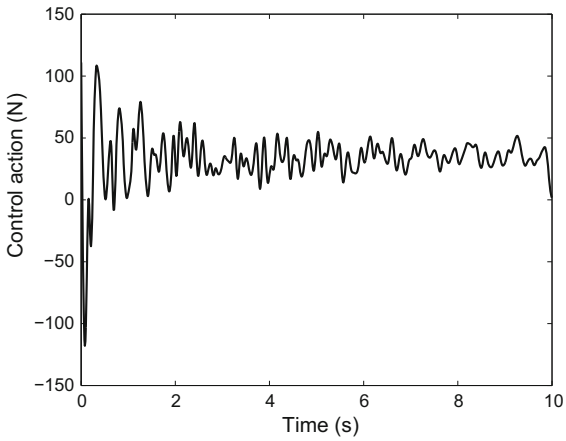

Fig. 4 Feedforward controller—u

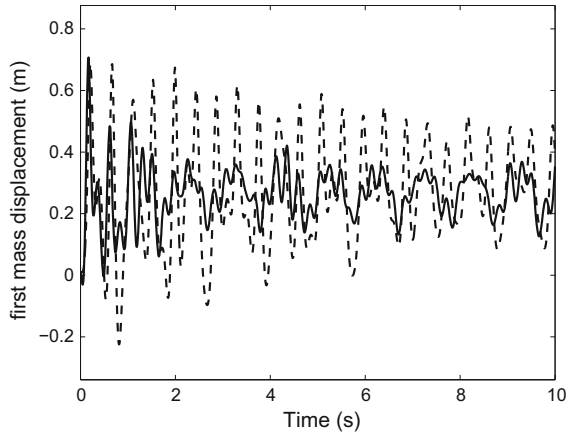

Fig. 5 Uncontrolled and controlled displacement (feedforward controller)—x_1

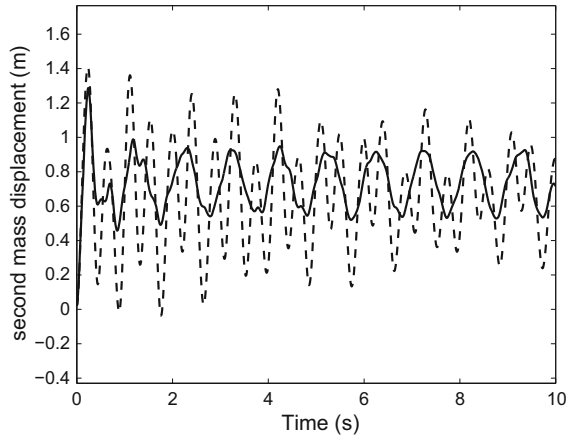

Fig. 6 Uncontrolled and controlled displacement (feedforward controller)—x_2

reduction of the system vibrations. The amplitude reductions of the system displacements can be assessed quantitatively by comparing the standard deviation values of the system displacements with and without the feedforward controller as follows:

$$\begin{cases} \lambda_{x_1} = \dfrac{\lambda_{x_1,u} - \lambda_{x_1,c}}{\lambda_{x_1,u}} = 50.392\% \\ \lambda_{x_2} = \dfrac{\lambda_{x_2,u} - \lambda_{x_2,c}}{\lambda_{x_2,u}} = 50.638\% \end{cases} \tag{39}$$

where $\lambda_{x_1,u}$, $\lambda_{x_2,u}$ denote the standard deviation values of the system displacements when there is no control action whereas $\lambda_{x_1,c}$, $\lambda_{x_2,c}$ denote the standard deviation values of the system displacements when the feedforward controller acts on the system. On the other

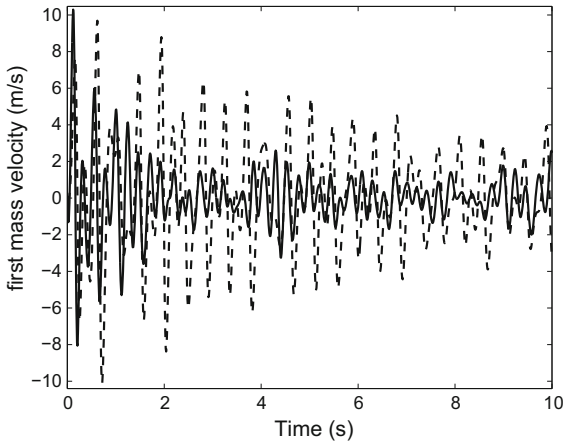

Fig. 7 Uncontrolled and controlled velocity (feedforward controller)—$\dot{x}_1$

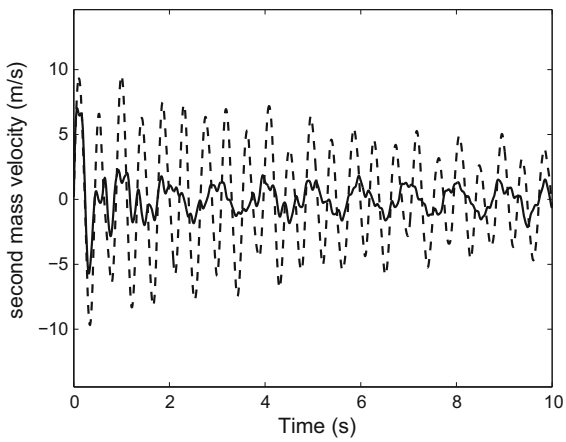

Fig. 8 Uncontrolled and controlled velocity (feedforward controller)—$\dot{x}_2$

hand, in Fig. 7 the dashed line depicts the velocity of the first mass when the system is uncontrolled while the solid line represents the velocity of the first mass when the feedforward controller acts on the system. In Fig. 8 the dashed line represents the velocity of the second mass when the system is uncontrolled whereas the solid line depicts the velocity of the second mass when the feedforward controller acts on the system. In this case, qualitatively these figures show that the action of the feedforward controller produces an appreciable amplitude reduction of the system vibrations. The amplitude reductions of both velocities can be evaluated quantitatively by comparing the standard deviation values of the system velocities with and without the feedforward controller as follows:

$$\begin{cases} \lambda_{\dot{x}_1} = \dfrac{\lambda_{\dot{x}_1,u} - \lambda_{\dot{x}_1,c}}{\lambda_{\dot{x}_1,u}} = 43.555\% \\ \lambda_{\dot{x}_2} = \dfrac{\lambda_{\dot{x}_2,u} - \lambda_{\dot{x}_2,c}}{\lambda_{\dot{x}_2,u}} = 65.987\% \end{cases} \tag{40}$$

where $\lambda_{\dot{x}_1,u}$, $\lambda_{\dot{x}_2,u}$ denote the standard deviation values of the system velocities when there is no control action while $\lambda_{\dot{x}_1,c}$, $\lambda_{\dot{x}_2,c}$ denote the standard deviation values of the system velocities when the feedforward controller acts on the system. Finally, in Fig. 9 the dashed line represents the interaction force when the system is uncontrolled whereas the solid line represents the interaction force when the feedforward controller acts on the system. Thus, the action of the feedforward controller yields a sensible amplitude reduction of the system interaction force, as shown in these figures. The amplitude reduction of the system interaction force can be estimated quantitatively by comparing the standard deviation values of the system interaction force with and without the feedforward controller as follows:

$$\lambda_\sigma = \frac{\lambda_{\sigma,u} - \lambda_{\sigma,c}}{\lambda_{\sigma,u}} = 70.510\% \tag{41}$$

where $\lambda_{\sigma,u}$ denotes standard deviation value of the system interaction force when there is no control action while $\lambda_{\sigma,c}$ denotes the standard deviation value of the system interaction force when the feedforward controller is applied on the mechanical system.

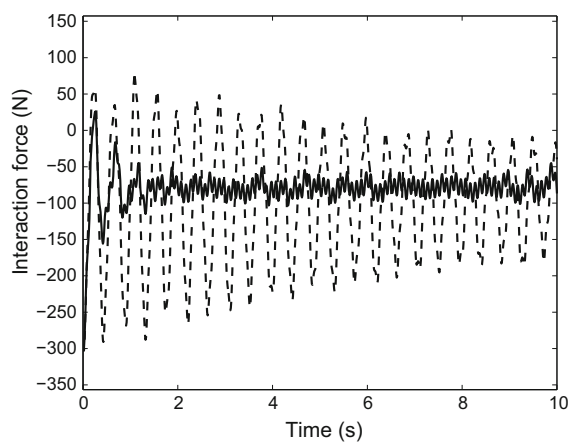

Fig. 9 Uncontrolled and controlled interaction force (feedforward controller)—σ

3.4 Feedback control design and development

In this subsection, the adjoint-based parameter optimization method is used to derive an optimal feedback controller and the numerical results obtained by means of the implementation of this type of control policy are shown.

The feedback controller described here is a closed-loop controller derived using the adjoint-based parameter optimization method. The control scheme which describes how the feedback controller acts on the mechanical system under consideration is represented in Fig. 10. Similarly to the feedforward controller, the goal of this feedback controller is to attenuate the amplitudes of the vibrations caused by the floating support and, at the same time, to attenuate more significantly the amplitude of the contact force between the second mass and the floating support which represents the interaction of the mechanical system with the external environment. Once the necessary system sensitivity matrices and vectors are identified following the same procedure described in the previous subsection, the adjoint-based parameter optimization method is implemented in order to derive an optimal feedback controller following the computational steps described in the paper. The resulting iterative convergence of the cost functional towards the minimum is represented in Fig. 11. This figure shows that in the case of the design of the feedback control action, the adjoint-based parameter optimization method converges very quickly to a minimum of the cost functional. The optimal feedback control action resulting from the adjoint-based parameter optimization method is represented in Fig. 12. The resulting optimal parameter vector for the proportional-derivative feedback controller is the following:

$$\gamma = \begin{bmatrix} -65.822 \\ 17.064 \end{bmatrix} \tag{42}$$

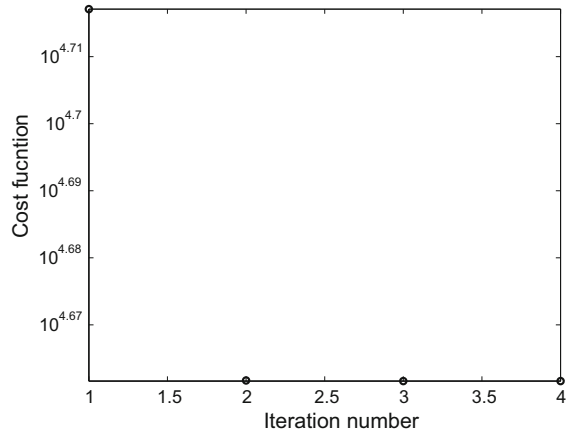

Fig. 11 Cost functional convergence for the feedback controller—J

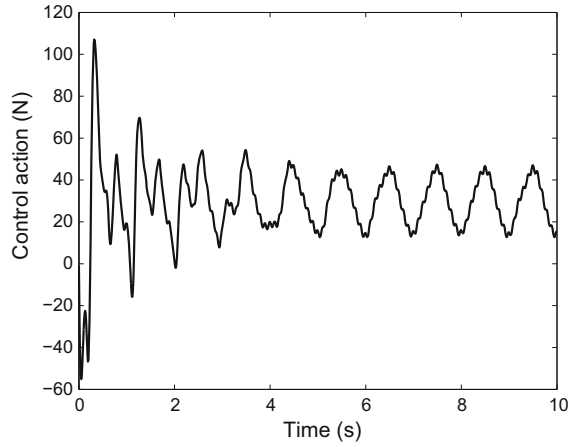

Fig. 12 Feedback controller—u

From a mathematical standpoint, these parameters identify respectively the coefficients of the proportional and derivative terms for the feedback controller. From a physical point of view, the first control parameter can be interpreted as a negative stiffness

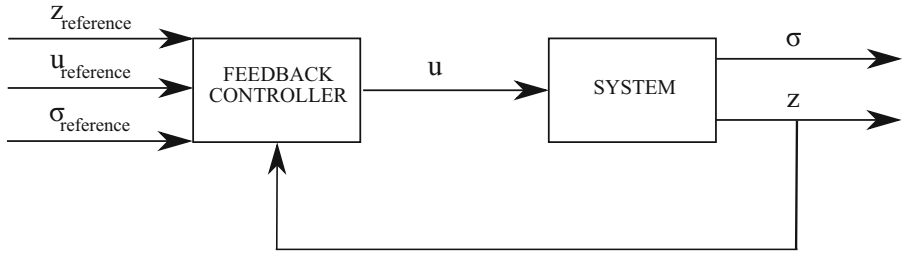

Fig. 10 Control scheme for feedback controller

coefficient while the second control parameter is analogous to a positive damping coefficient. In Fig. 13 the dashed line represents the displacement of the first mass when the system is uncontrolled whereas the solid line depicts the displacement of the first mass when the feedback controller acts on the system. In Fig. 14 the dashed line depicts the displacement of the second mass when the system is uncontrolled while the solid line represents the displacement of the second mass when the feedback controller acts on the system. From a qualitative point of view, these figures show that the outcome of the feedback control action is a considerable amplitude attenuation of the system vibrations. The amplitude attenuations of the system displacements can be evaluated quantitatively by comparing the standard deviation values of the system displacements with and without the feedback controller as follows:

$$\begin{cases} \lambda_{x_1} = \dfrac{\lambda_{x_1,u} - \lambda_{x_1,c}}{\lambda_{x_1,u}} = 45.261\% \\ \lambda_{x_2} = \dfrac{\lambda_{x_2,u} - \lambda_{x_2,c}}{\lambda_{x_2,u}} = 44.705\% \end{cases} \tag{43}$$

where $\lambda_{x_1,u}$, $\lambda_{x_2,u}$ denote the standard deviation values of the system displacements when there is no control action whereas $\lambda_{x_1,c}$, $\lambda_{x_2,c}$ denote the standard deviation values of the system displacements when the feedback controller acts on the system. On the other hand, in Fig. 15 the dashed line depicts the velocity of the first mass when the system is uncontrolled while the solid line represents the velocity of the first mass when the feedback controller acts on the system. In

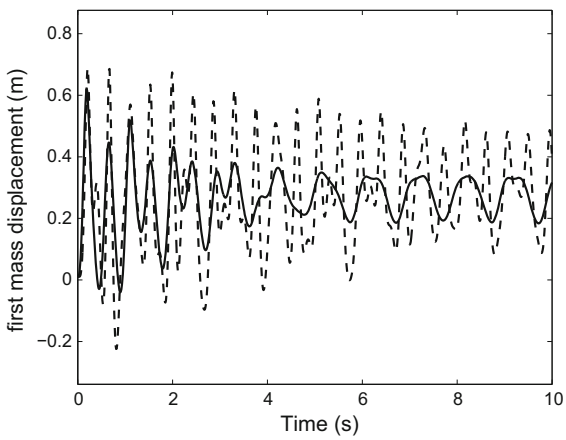

Fig. 13 Uncontrolled and controlled displacement (feedback controller)—x_1

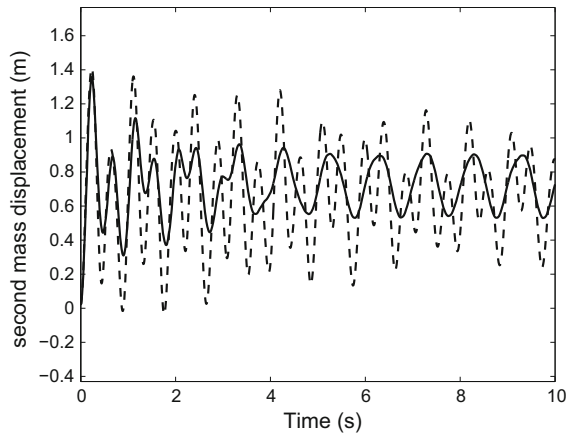

Fig. 14 Uncontrolled and controlled displacement (feedback controller)—x_2

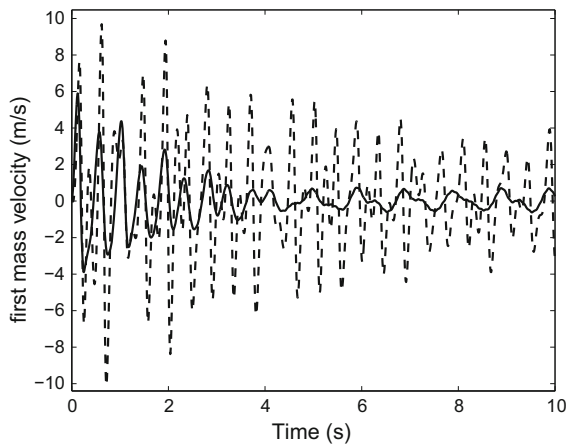

Fig. 15 Uncontrolled and controlled velocity (feedback controller)—$\dot{x}_1$

Fig. 16 the dashed line represents the velocity of the second mass when the system is uncontrolled whereas the solid line depicts the velocity of the second mass when the feedback controller acts on the system. In this case, qualitatively these figures show that the feedback controller yields a considerable attenuation of the system vibrations. The attenuations of both velocities can be assessed quantitatively by comparing the standard deviation values of the system velocities with and without the feedback controller as follows:

$$\begin{cases} \lambda_{\dot{x}_1} = \dfrac{\lambda_{\dot{x}_1,u} - \lambda_{\dot{x}_1,c}}{\lambda_{\dot{x}_1,u}} = 60.466\% \\ \lambda_{\dot{x}_2} = \dfrac{\lambda_{\dot{x}_2,u} - \lambda_{\dot{x}_2,c}}{\lambda_{\dot{x}_2,u}} = 57.429\% \end{cases} \tag{44}$$

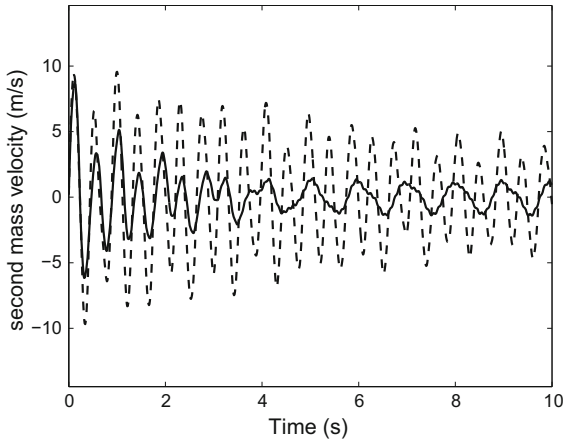

Fig. 16 Uncontrolled and controlled velocity (feedback controller)—$\dot{x}_2$

where $\lambda_{\dot{x}_1,u}$, $\lambda_{\dot{x}_2,u}$ denote the standard deviation values of the system velocities when there is no control action while $\lambda_{\dot{x}_1,c}$, $\lambda_{\dot{x}_2,c}$ denote the standard deviation values of the system velocities when the feedback controller acts on the system. Finally, in Fig. 17 the dashed line represents the interaction force when the system is uncontrolled whereas the solid line represents the interaction force when the feedback controller acts on the system. Therefore, the effect of the feedback controller is a remarkable attenuation of the system interaction force, as shown in these figures. The amplitude attenuation of system interaction force can be estimated quantitatively by comparing the standard deviation values of the system interaction force with and without the feedback controller as follows:

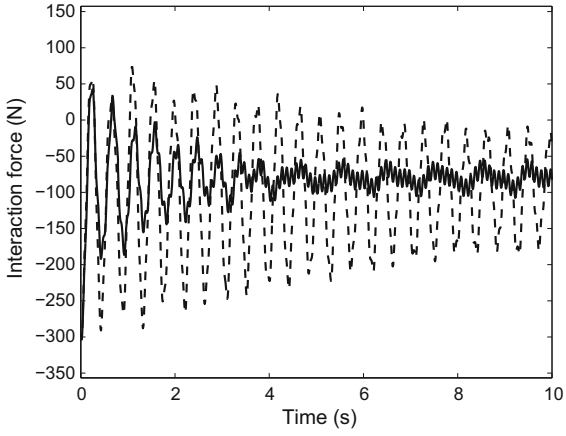

Fig. 17 Uncontrolled and controlled interaction force (feedback controller)—σ

$$\lambda_\sigma = \frac{\lambda_{\sigma,u} - \lambda_{\sigma,c}}{\lambda_{\sigma,u}} = 58.458\% \tag{45}$$

where $\lambda_{\sigma,u}$ denotes standard deviation value of the system interaction force when there is no control action while $\lambda_{\sigma,c}$ denotes the standard deviation value of the system interaction force when the feedback controller is applied on the mechanical system.

4 Summary, conclusions, and recommendations for future research

The primary research objective of the authors is to develop new, effective and efficient methods to perform accurate analytic modeling [67–72] experimental parameter identification [73–76], and numerical control optimization [77–80] of rigid as well as flexible mechanical systems exploiting the deep connections between multibody dynamics, system identification, and control theory. In particular, this paper is an analytical as well as a numerical investigation on the use of adjoint method for the optimal design of control policies for reducing the nonlinear vibrations of mechanical systems.

In this paper, the optimal control problem was addressed and solved by developing two novel control algorithms, namely the iterative adjoint-based control optimization method and the iterative adjoint-based parameter optimization method. These dual numerical procedures proposed in the paper were designed in order to implement the active and passive control paradigms for the suppression of the structural vibrations of nonlinear dynamical systems and, simultaneously, for the attenuation of the contact forces which result from the interaction of a mechanical system with the external environment. Indeed, this investigation represents an attempt to put in a unified framework a new set of computational methods that can be employed to design effectively hybrid motion-force control strategies for nonlinear mechanical systems. The crucial aspects of the adjoint-based optimization methods were reviewed in this work, paying particular attention to the optimal design of feedforward and feedback control laws for nonlinear mechanical systems. To this end, a concise review of the optimal control theory based on the calculus of variation and on the adjoint equations was given in the paper. Then, detailed descriptions of the adjoint-based control

optimization method and of the adjoint-based parameter optimization method were reported. The proposed numerical procedures were applied to design a feedforward controller and a feedback controller aimed at realizing the suppression of the structural vibrations and, at the same time, the attenuation of the contact forces for a simple but illustrative nonlinear underactuated mechanical system. For the sake of a clear description of the proposed computational methods, the dynamical system analyzed in the paper is a simple two degrees of freedom lumped-parameter mechanical system featuring a nonlinear elastic force field. The system equations of motion were explicitly derived together with the state function sensitivity matrices in order to show the necessary steps to implement the proposed adjoint-based optimization procedures. The nonlinear mechanical system considered in the paper as a case study interacts with the external environment and it is excited by a moving support. Thus, the force between the system and the floating support is considered as a smooth contact force. A control device is collocated between the two vibrating masses in order to attenuate the magnitude of the contact force and, simultaneously, mitigate the amplitude of the nonlinear mechanical vibrations. To this end, a quadratic structure was adopted for the mathematical form of the cost functional and the cost functional sensitivity vectors necessary to implement the two proposed adjoint-based optimization procedures were explicitly calculated. By means of numerical simulations, the syntheses of an optimal feedforward controller and of an optimal feedback controller were obtained together with the corresponding time histories of the system state. The set of numerical results obtained in this work shows a considerable attenuation of the amplitude of the mechanical vibrations and of the magnitude of the interaction forces, thereby demonstrating the effectiveness of the proposed computational procedures.

Although the numerical results presented in this paper are obtained employing a lumped-parameter model of an illustrative nonlinear mechanical system, the adjoint-based optimization method developed in this investigation is also applicable for controlling the structural vibration of distributed-parameter systems. To this end, a finite set of nonlinear ordinary differential equations can be obtained for modeling the dynamic equations of a continuous mechanical system using approximation methods. Approximation methods for the discretization of the spatial dimensions are, for instance, the classical Rayleigh-Ritz technique, the Galerkin method, or the finite element method [81]. In all the approximation methods cited before, the position field of a continuum body is expressed from the outset in a manner consistent with the body boundary conditions using a linear combination of a given set of base functions and a corresponding number of time-dependent coordinates. Subsequently, the system equations of motions are obtained from the assumed kinematic description employing the fundamental principles of continuum mechanics [82]. However, the traditional Rayleigh–Ritz technique and the classical Galerkin method have two undesirable properties. First, the assumed displacement fields must be selected accurately and eventually adjusted to match the boundary conditions of the continuum body. This task is challenging for complex three-dimensional geometry and it is left to the analyst. Second, in the classical discretization techniques, the generalized coordinates lack an obvious physical meaning. In the kinematic formulation of the finite element method, on the other hand, these difficulties are overcome by using a set of generalized coordinates that describe displacements, slopes, and curvatures at given nodal locations and form the basic unknown of the problem. The finite element method can be considered as a special case of the Galerkin technique in which the continuum body is separated into a certain number of finite elements interconnected at the nodal points located on the element boundaries [83]. Furthermore, simple interpolating polynomials are used in the finite element method to adequately describe the position field within the element [84]. Therefore, the finite element method is more advantageous for practical engineering applications and leads to a discrete set of dynamic equations which can be formulated and solved in a systematic manner. Since the adjoint-based procedure developed in this work assumes a general nonlinear form of the system equations of motion featuring the structure of a set of ordinary differential equations, this methodology is applicable to discrete lumped-parameter models of mechanical systems as well as to discrete models of distributed-parameter mechanical systems obtained using the finite element method. More specifically, the among all the finite element formulation available, the absolute nodal coordinate formulation (ANCF) is particularly attractive for the application of the

proposed adjoint-based numerical procedures [85]. In the absolute nodal coordinate formulation, a unique kinematic representation is used to represent the displacement field as well as the rotation field of a general continuum body performing a separation of space-dependent variables and time-dependent coordinates. In particular, one of the distinguishing features of this finite element formulation is the use of global positions and position vector gradients as nodal coordinates. Consequently, finite elements based on the absolute nodal formulation have a constant mass matrix, leads to zero centrifugal and Coriolis generalized inertia forces, and can correctly describe rigid body motion [86]. Furthermore, the use of slope vectors as generalized coordinates in the absolute nodal coordinate formulation facilitates the development of complex curved geometry and allows for the implementation of a non-incremental solution procedure for the numerical solution of the equations of motion [87]. All the desirable properties of the absolute nodal coordinate formulation mentioned before will pave the way towards the application of the adjoint-based control and parameter optimization procedures developed in this paper to complex distributed-parameter systems.

An important issue that needs further investigation is the performance of the adjoint-based control and parameter optimization procedures for nonlinear mechanical systems working in a noisy environment. Additional complexity is added to this realistic scenario when only incomplete information is available for the system state. For instance, in vehicle engineering applications, mechanical components perform large translations, undergo finite rotations, can deform in a nonlinear fashion, vibrate under the effect of cyclic loading, and are affected by stochastic disturbances originated by the interaction with the external environment [88–91]. Furthermore, the actual control devices implemented on a mechanical system have a limited actuation power and need to deal with a finite set of signals affected by process noise and measurement uncertainties [92, 93]. Further examples in which taking into account the stochastic nature of the operational space is particularly important are mechanical system subjected to nanometric oscillations. Indeed, nanometer oscillations are characterized by length scales where the random behavior play a crucial role. The optimal design of control strategies for nanoscopic systems with complex nonlinearities and noise effects, such as polymers under the applications of force fields, can represent an area of pioneering research [94, 95]. In all these challenging scenarios, however, a simple and effective strategy can be employed to design robust control actions based on the adjoint procedure developed in this investigation exploiting, for instance, the well-known linear-quadratic-Gaussian control and estimation method (LQG) [96]. To this end, a nominal model of the mechanical system under study is first developed assuming an unlimited amount of resources for the control action and a full sensing of the system state. The resulting evolution of the mechanical system is then assumed as a reference trajectory for the dynamic evolution of the system state and the corresponding control action is considered as a feedforward control signal. Subsequently, a feedback controller based on a linear model of the mechanical system obtained linearizing around the precomputed trajectory is designed to compensate the difference in the dynamical behavior of the nominal system and the actual system. For this purpose, a nonlinear observer is designed to estimate the state of the actual system using the available measurements employing a Kalman filter approach [97]. In the authors' viewpoint, the combination of the adjoint-based optimization procedures with the linear-quadratic-Gaussian control and estimation techniques represents a promising method for the control of nonlinear underactuated mechanical systems characterized by process disturbances, measurement uncertainty, and incomplete state information.

To conclude, the authors are of the opinion that the adjoint-based control optimization method and the adjoint-based parameter optimization method represent efficient and effective strategies to control nonlinear underactuated mechanical systems that successfully achieve a hybrid motion-force control paradigm. Future research efforts will be dedicated to the analytical development and to the numerical implementation of the adjoint method for the active and passive optimal control design in the case of more complex mechanical systems, such as the rigid and flexible multibody systems that are mathematically modelled by a set of differential-algebraic equations of motion [98–101]. Furthermore, future work will be dedicated to performing a systematic comparison between the nonlinear control method developed in this investigation and other modern control strategies

that can be generally applied to lumped-parameter systems as well as to distributed-parameter systems. To this end, particular attention will be devoted to the use of the fundamental equations of constrained motion recently developed by Udwadia and Kalaba in the field of analytical dynamics [102–104]. Similarly to the adjoint-based control optimization procedure analyzed in this investigation, the Udwadia–Kalaba equations can be employed to derive closed-form expressions of nonlinear control forces for nonlinear mechanical systems without imposing an a priori structure on the nonlinear controller [105–107]. Using the Udwadia–Kalaba approach, optimal control policies for nonlinear mechanical systems are designed formulating a set of holonomic or nonholonomic constraint equations and the corresponding generalized constraint forces are interpreted as control actions [108–110]. Since in numerous investigations was demonstrated that the Udwadia–Kalaba method is general and effective, a comparison with the adjoint-based approach for optimal control developed by the authors will be investigated in future publications.

Compliance with ethical standards

Conflict of interest The authors declare that they have no conflict of interest.

References

1. Nayfeh AH, Mook DT (1995) Nonlinear oscillations. Wiley, New York
2. Khalil HK (2001) Nonlinear systems, 3rd edn. Prentice Hall, Upper Saddle River
3. Antman SS (2005) Nonlinear problems of elasticity, 2nd edn. Springer, New York
4. Meirovitch L (2010) Fundamentals of vibrations. McGraw Hill, Boston
5. Hagedorn P, DasGupta A (2007) Vibrations and waves in continuous mechanical systems. Wiley, Chichester
6. Preumont A (2011) Vibration control of active structures: an introduction, 3rd edn. Springer, Berlin
7. Bauchau OA, Craig JI (2009) Structural analysis: with applications to aerospace structures. Springer, New York
8. Hodges DH, Pierce GA (2002) Introduction to structural dynamics and aeroelasticity. Cambridge University Press, Cambridge
9. Genta G (2009) Vibration dynamics and control. Springer, New York
10. Inman DJ (2006) Vibration with control. Wiley, Chichester
11. Slotine JE, Li W (1991) Applied nonlinear control. Prentice Hall, Englewood Cliffs
12. Cheli F, Diana G (2015) Advanced dynamics of mechanical systems. Springer, London
13. Gawronski WK (2004) Advanced structural dynamics and active control of structures. Springer, New York
14. Skelton RE, de Oliveira MC (2009) Tensegrity systems. Springer, New York
15. Juang JN, Phan MQ (2004) Identification and control of mechanical systems. Cambridge University Press, Cambridge
16. Seifried R (2014) Dynamics of underactuated multibody systems: modeling, control and optimal design. Springer, London
17. Zhong WX (2004) Duality system in applied mechanics and optimal control. Kluwer Academic Publishers, New York
18. Inman DJ (2008) Engineering vibration, 3rd edn. Prentice Hall, Upper Saddle River
19. Al Majid A, Dufour R (2002) Formulation of a hysteretic restoring force model: application to vibration isolation. J Nonlinear Dyn 27:69–85
20. Ashour ON, Nayfeh AH (2002) Adaptive control of flexible structures using a nonlinear vibration absorber. J Nonlinear Dyn 28:309–322
21. Siciliano B, Sciavicco L, Villani L, Oriolo G (2010) Robotics: modelling, planning and control. Springer, London
22. Bryson AE, Ho YC (1975) Applied optimal control: optimization, estimation and control. Taylor and Francis, New York
23. Luchini P, Bottaro A (2014) An introduction to adjoint problems. Annu Rev Fluid Mech 46(1):493
24. Luchini P, Bottaro A (2014) Adjoint equations in stability analysis. Annu Rev Fluid Mech 46:1–30
25. Bewley TR (2015) Numerical renaissance: simulation, optimization and control. Renaissance Press, To be published
26. Bertsekas DP (2005) Dynamic programming and optimal control—volume 1. Athena Scientific, Belmont
27. Bertsekas DP (2005) Dynamic programming and optimal control—volume II. Athena Scientific, Belmont
28. Bellman RE, Dreyfus SE (1962) Applied dynamic programming. Oxford University Press, London
29. Bewley TR (2001) Flow control: new challenges for a new eenaissance. Prog Aerosp Sci 37:21–58
30. Kim J, Bewley TR (2007) A linear systems approach to flow control. Annu Rev Fluid Mech 39:383–417
31. Giles MB, Pierce NA (2000) An introduction to the adjoint approach to design. J Flow Turbul Combust 65:393–415
32. Giannetti F, Luchini P (2006) Leading-edge receptivity by adjoint methods. J Fluid Mech 547:21–53
33. Giannetti F, Camarri S, Luchini P (2010) Structural sensitivity of the secondary instability in the wake of a circular cylinder. J Fluid Mech 651:319–337
34. Luchini P, Bewley TR (2010) Methods for the solution of very large flow-control problems that bypass open-loop model reduction. Bull Am Phys Soc 55–16:42–42
35. Schmidt-Wetekam C, Zhang D, Hughes R, Bewley TR (2007) Design, optimization, and control of a new class of reconfigurable hopping rovers. In: Proceedings of the 46th IEEE conference on decision and control New Orleans, December 12–14

36. Summers S, Bewley TR (2007) MPDopt: a versatile toolbox for adjoint-based model predictive control of smooth and switched nonlinear dynamic systems. In: Proceedings of the 46th IEEE conference on decision and control New Orleans, December 12–14
37. Bewley TR, Temam R, Zianed M (2000) A general framework for robust control in fluid mechanics. Phys D Nonlinear Phenom 138(3–4):360–392
38. Raibert MH, Craig JJ (1981) Hybrid position-force control of manipulators. J Dyn Syst Meas Control 103(2):126–133
39. Gorinevsky D, Formalsky A, Schneider A (1997) Force control of robotics systems. CRC Press, Boca Raton
40. Spong MW, Hutchinson S, Vidyasagar M (2005) Robot modeling and control. Wiley, New York
41. Lewis FL, Dawson DM, Abdallah CT (2003) Robot manipulator control: theory and practice. CRC Press, Boca Raton
42. Guida D, Pappalardo CM (2015) Control design of an active suspension system for a quarter-car model with hysteresis. J Vib Eng Technol 3(3):277–299
43. Guida D, Pappalardo CM (2013) Development of a closed-chain multibody model of a high-speed railway pantograph for hybrid motion/force control of the pantograph/catenary interaction. J Mech Eng Ind Des 3(5):45–85
44. Ogata K (2010) Modern control engineering, 5th edn. Prentice Hall, Boston
45. Guida D, Pappalardo CM (2013) Swing-up and stabilization of an inverted pendulum with dry friction. J Mech Eng Ind Des 2(5):40–56
46. Vincent TL, Grantham JW (1997) Nonlinear and optimal control systems. Wiley, New York
47. Betts JT (2010) Practical methods for optimal control and estimation using nonlinear programming, 2nd edn. Siam, Philadelphia
48. Clarke F (2013) Functional analysis, calculus of variation and optimal control. Springer, London
49. Stengel RF (1986) Optimal control and estimation. Dover, New York
50. Bement MT, Bewley TR (2008) Excitation design for damage detection using iterative adjoint-based optimization—Part 1: method development. Mech Syst Signal Process 23:783–793
51. Nise NS (2011) Control system engineering, 6th edn. Wiley, New York
52. Troutman JL (1995) Variational calculus and optimal control: optimization with elementary convexity, 2nd edn. Springer, New York
53. Liberzon D (2012) Calculus of variations and optimal control theory: a concise introduction. Princeton University Press, Princeton
54. Lewis FL, Vrabie DL, Syrmos VL (2012) Optimal control, 3rd edn. Wiley, New York
55. Bement MT, Bewley TR (2008) Excitation design for damage detection using iterative adjoint-based optimization—Part 2: experimental demonstration. Mech Syst Signal Process 23:794–803
56. Kirk DE (1970) Optimal control theory: an introduction. Dover, Mineola
57. Guida D, Pappalardo CM (2013) Optimal control design of an active mass damper with dry friction. J Mech Eng Ind Des 2(4):27–39
58. Press WH, Teukolsky SA, Vetterling WT, Flannery BP (2007) Numerical recipes: the art of scientific computing, 3rd edn. Cambridge University Press, Cambridge
59. Guida D, Pappalardo CM (2013) A new method for control law design of a quarter-car suspension system. J Mech Eng Ind Des 1(5):37–58
60. Snyman JA (2005) Practical mathematical optimization: an introduction to basic optimization theory and classical and new gradient-based algorithms. Springer, New York
61. Shabana AA (2013) Dynamics of multibody systems, Forth edn. Cambridge University Press, Cambridge
62. Meirovitch L (2010) Methods of analytical dynamics. Dover, Mineola
63. Lanczos C (1986) The bariational principles of mechanics, 4th edn. Dover, Mineola
64. Goldstein H, Poole CP, Safko JL (2013) Classical mechanics, 3rd edn. Addison Wesley, San Francisco
65. Fantoni I, Lozano R (2001) Non-linear control for underactuated mechanical systems. Springer, London
66. Guida D, Pappalardo CM (2014) Forward and inverse dynamics of nonholonomic mechanical systems. Meccanica 49(7):1547–1559
67. Pappalardo CM (2015) A natural absolute coordinate formulation for the kinematic and dynamic analysis of rigid multibody systems. J Nonlinear Dyn 81(4):1841–1869
68. Pappalardo CM, Patel MD, Tinsley B, Shabana AA (2015) Contact force control in multibody pantograph/catenary systems. In: Proceedings of the institution of mechanical engineers, Part K: journal of multibody dynamics, pp 1–22
69. Pappalardo CM, Yu Z, Zhang X, Shabana AA (2015) Rational ANCF thin plate finite element. J Comput Nonlinear Dyn 11(5):1–15
70. Kulkarni S, Pappalardo CM, Shabana AA (2017) Pantograph/catenary contact formulations. ASME J Vib Acoust 139(1):1–12
71. Pappalardo CM, Wallin M, Shabana AA (2017) A new ANCF/CRBF fully parametrized plate finite element. ASME J Comput Nonlinear Dyn 12(3):1–13
72. Guida D, Nilvetti F, Pappalardo CM (2012) Modelling, identification and control of a three-story building system. J Mech Eng Ind Des 1(3):36–60
73. Guida D, Pappalardo CM (2009) Sommerfeld and mass parameter identification of lubricated journal bearing. WSEAS Trans Appl Theor Mech 4(4):205–214
74. Guida D, Nilvetti F, Pappalardo CM (2009) Parameter identification of a two degrees of freedom mechanical system. Int J Mech 3(2):23–30
75. Guida D, Nilvetti F, Pappalardo CM (2010) Parameter identification of a full-car model for active suspension design. J Achiev Mater Manuf Eng 40(2):138–148
76. Nilvetti F, Pappalardo CM, Guida D (2012) Mass, stiffness and damping identification of a two-story building model. J Mech Eng Ind Des 1(2):19–35
77. Guida D, Nilvetti F, Pappalardo CM (2009) Instability induced by dry friction. Int J Mech 3(3):44–51

78. Guida D, Nilvetti F, Pappalardo CM (2009) Dry friction inuence on cart pendulum dynamics. Int J Mech 3(2):31–38
79. Guida D, Nilvetti F, Pappalardo CM (2010) Dry friction of bearings on dynamics and control of an inverted pendulum. J Achiev Mater Manuf Eng 38(1):80–94
80. Guida D, Pappalardo CM (2013) A new control algorithm for active suspension systems featuring hysteresis. FME Trans 41(4):285–290
81. Marsden JE, Hughes TJR (1994) Mathematical foundations of elasticity. Dover, New York
82. Meirovitch L (1980) Computational methods in structural dynamics. Springer, Netherlands
83. Bathe JK (2007) Finite element procedures. Prentice Hall, Upper Saddle River, New Jersey
84. Hughes TJR (1987) The finite element method: linear static and dynamic finite element analysis. Prentice Hall, Englewood Cliffs
85. Shabana AA (2012) Computational continuum mechanics, 2nd edn. Cambridge University Press, Cambridge
86. Shabana AA (2015) Definition of ANCF finite elements. ASME J Comput Nonlinear Dyn 10(5):1–5
87. Belytschko T, Liu WK, Moran B, Elkhodary KI (2013) Nonlinear finite elements for continua and structures, 2nd edn. Wiley, Hoboken
88. Wong JY (2009) Terramechanics and off-road vehicle engineering: terrain behaviour, off-road vehicle performance, and design, 2nd edn. Butterworth-Heinemann, Oxford
89. Pacejka H (2012) Tire and vehicle dynamics, 3rd edn. Butterworth-Heinemann, Oxford
90. Blundell M, Harty D (2014) Multibody systems approach to vehicle dynamics, 2nd edn. Butterworth-Heinemann, Oxford
91. Shabana AA, Zaazaa KE, Sugiyama H (2008) Railroad vehicle dynamics: a computational approach. CRC Press - Taylor and Francis, Boca Raton
92. Rajamani R (2012) Vehicle dynamics and control, 2nd edn. Springer, New York
93. Crassidis JL, Junkins JL (2011) Optimal estimation of dynamic systems, 2nd edn. CRC Press - Taylor and Francis, Boca Raton
94. Manca F, Giordano S, Palla PL, Zucca R, Cleri F, Colombo L (2012) Theory and Monte Carlo simulations for the stretching of flexible and semiflexible single polymer chains under external fields. J Chem Phys 136:1–11
95. Manca F, Giordano S, Palla PL, Zucca R, Cleri F, Colombo L (2012) Theory and Monte Carlo simulations for the stretching of flexible and semiflexible single polymer chains under external fields. J Chem Phys 137:1–13
96. Lewis FL, Xie L, Popa D (2008) Optimal and robust estimation: with an introduction to stochastic control theory, 2nd edn. CRC Press - Taylor and Francis, Boca Raton
97. Brown RG, Hwang PYC (2012) Introduction to random signals and applied Kalman filtering with MATLAB exercises, 4th edn. Wiley, Hoboken
98. Nikravesh PE (1988) Computer-aided analysis of mechanical systems. Prentice Hall, Englewood Cliffs
99. Haug EJ (1989) Computer aided kinematics and dynamics of mechanical systems. Volume I: basic methods. Allyn and Bacon, Needham
100. Cheli F, Pennestri E (2006) Cinematica e dinamica dei sistemi multibody, volume 1. Casa Editrice Ambrosiana, Milano
101. Cheli F, Pennestri E (2006) Cinematica e dinamica dei sistemi multibody, volume 2. Casa Editrice Ambrosiana, Milano
102. Udwadia FE, Kalaba RE (2007) Analytical dynamics: a new approach. Cambridge University Press, Cambridge
103. Udwadia FE, Kalaba RE, De Falco D (2009) Dinamica analitica. Un nuovo approccio. Edises, Napoli
104. Udwadia FE (2016) Constrained motion of Hamiltonian systems. J Nonlinear Dyn 84:11351145
105. Koganti PB, Udwadia FE (2016) Unified approach to modeling and control of rigid multibody systems. J Guid Control Dyn 39(12):2683–2698
106. Udwadia FE (2016) Inverse problem of Lagrangian mechanics for classically damped linear multi-degrees-of-freedom systems. ASME J Appl Mech 83(10):1–4
107. Udwadia FE, Koganti PB (2015) Optimal stable control for nonlinear dynamical systems: an analytical dynamics based approach. J Nonlinear Dyn 82(1–2):547–562
108. Udwadia FE, Wanichanon T (2015) Control of uncertain nonlinear multibody mechanical systems. ASME J Appl Mech 81(4):1–11
109. Pappalardo CM (2012) Combination of extended Udwadia–Kalaba control algorithm with extended Kalman filter estimation method. J Mech Eng Ind Des 1(1):1–18
110. Guida D, Pappalardo CM (2012) A new control algorithm for nonlinear underactuated mechanical systems. J Mech Eng Ind Des 1(4):61–82